Spectral Analysis of High-Frequency Finance

by

Yuqing Zhang

Submitted to the Department of Electrical Engineering and Computer Science
in partial fulfillment of the requirements for the degree of

Master of Engineering in Electrical Engineering and Computer Science

at the

MASSACHUSETTS INSTITUTE OF TECHNOLOGY

June 2016

Author .....
Department of Electrical Engineering and Computer Science
May 20, 2016

Certified by .....
Andrew W. Lo
Charles E. and Susan T. Harris Professor
Thesis Supervisor

Accepted by .....
Christopher J. Terman
Chairman, Masters of Engineering Thesis Committee

Spectral Analysis of High-Frequency Finance

by

Yuqing Zhang

Submitted to the Department of Electrical Engineering and Computer Science
on May 20, 2016, in partial fulfillment of the
requirements for the degree of
Master of Engineering in Electrical Engineering and Computer Science

Abstract

Popular across a wide range of fields, spectral analysis is a powerful technique for studying the behavior of complex systems. It decomposes a signal into many different periodic components, each associated with a specific cycle length. We argue that the application of spectral analysis to finance leads to natural interpretations in terms of horizon-specific behaviors. A spectral framework provides a few main advantages over conventional time domain approaches to financial analysis: (1) improved computational efficiency for the evaluation of behaviors across a spectrum of time horizons, (2) reduced vulnerability to aliasing effects, and (3) more convenient representations of inherently cyclic dynamics, e.g. business cycles, credit cycles, liquidity cycles, etc.

In this paper we first present a set of spectral techniques, including a frequency-specific correlation and a frequency decomposition of trading strategy profits. Then, we demonstrate the application of these techniques in an empirical analysis of high-frequency dynamics over the years 1995-2014. Our results consist of three parts: (1) an analysis of individual stock returns and various portfolio returns, (2) an analysis of contrarian trading strategies and the introduction of a novel technique for managing frequency exposures of general strategies, and (3) a case analysis of recent market shocks. The great extent to which our empirical results align with financial intuition attests to the practicality of spectral approaches to financial analysis. It demonstrates that many real phenomena can be captured through a spectral lens.

Thesis Supervisor: Andrew W. Lo
Title: Charles E. and Susan T. Harris Professor

Acknowledgments

I deeply thank all of my family, friends, teachers, and mentors for their encouragement, their wisdom, and their inspiration throughout my life. I have been profoundly influenced by a great many individuals, and I feel exceptionally fortunate to have spent (and continue to spend) my growing years in their company.

I am deeply grateful to my mother Yehong and my father Guosen, who have surmounted incredible challenges in building a better world for me. It goes without saying that this work would not have been realized without them. I thank my sister Yushu, for whom I aspire to be a role model, for keeping me young. I thank my best friend Claire, with whom I have grown immensely over the past few years, for blessing me with her support and her optimism.

I would like to thank Prof. Andrew W. Lo for his guidance, his insights, and his time. I thoroughly thank Shomesh Chaudhuri, whose research has laid the groundwork for this thesis, for his endless willingness to teach, share, and explore. Finally, I thank Jayna and Allie for making many crucial resources available.

Contents

List of Figures and Tables

Chapter 1

Introduction

Spectral analysis is a powerful technique for studying the behavior of complex systems. Also known as frequency domain analysis, its fields of application are extraordinarily wide, ranging from engineering to chemistry to astronomy. Spectral analysis allows us to decompose signals and systems into periodic components across a range of cycle lengths, known as a frequency decomposition, and often leads to more convenient system representations. This technique is especially useful when the individual components in the decomposition can be assigned practical meaning in the context of the application.

One might argue that a frequency domain perspective of financial processes is naturally intuitive – each periodic component in the frequency decomposition reflects dynamics along the specific investment horizon corresponding to the cycle length. Spectral analysis is potentially an extremely useful tool for studying horizon-specific market characteristics, because the frequency decomposition allows us to isolate horizon-specific components of financial quantities.

A main advantage of our proposed spectral framework, compared to traditional time-domain techniques, is that it is less susceptible to aliasing effects (discussed in Section 2.3.3). We argue that a spectral framework is better equipped to leverage the full granularity of available data. In addition, inherently cyclic dynamics (e.g. business cycles, credit cycles, liquidity cycles) can be more conveniently represented in the frequency domain. At the very least, spectral methods allow more computationally

efficient analysis across a continuous spectrum of time horizons.

In this paper we study intraday dynamics over the years 1995-2014, a period marked by the rise of technology and the resulting growth of high-frequency activity. As the spectrum of relevant time horizons has widened over the past two decades, it has become increasingly important to understand horizon-specific dynamics. We present techniques, along with corresponding empirical results, for analyzing the frequency-specific behavior of individual returns (stocks and portfolios), pairs of returns, and trading strategies.

Chapter 1 introduces background material and describes our data set in detail. Chapter 2 presents our spectral analysis techniques and delivers an intuitive commentary motivated by financial applications. Chapter 3 summarizes empirical results for a frequency-domain analysis of stock and portfolio returns. Chapter 4 studies the empirical spectral properties of contrarian trading strategies over the S&P 1500. Chapter 5 provides an analysis of recent market shocks through a spectral lens, attempting to shed light on the ways in which these shocks have altered the market. Finally, in Chapter 6 we conclude and suggest future work.

1.1 Horizon-specific Market Characteristics

In this section we motivate the application of spectral analysis to finance. We examine the financial markets across time horizons, highlighting horizon-specific characteristics in returns behavior and market participants. As these horizon-based distinctions have grown increasingly prominent over the past two decades, the development of tools for studying these horizon-specific behaviors is now more important than ever. We propose spectral analysis as one such tool.

Ever since the inception of the modern financial system, its characteristics have drawn the attention of many. A particularly popular (and profitable) problem is understanding the behavior of financial returns. Because the financial markets evolve quickly, it is difficult for empirical studies to reach definitive conclusions. However, a great body of literature suggests that financial returns behave differently along

different time horizons. Here we provide a very brief summary of results.

There is evidence that asset returns along horizons of at least one month are driven by fundamental and macroeconomic factors. In the early 1990s, Fama and French argued that cross-sectional variance in average stock returns can be significantly attributed to fundamental factors [24] [25]. They discovered that small cap stocks and value stocks (stocks with high book-to-market ratios) tend to outperform the rest of the market on a monthly basis. Other fundamental quantities like company profitability and earnings have also been suggested to hold predictive value [51] [8] [55]. In 1999, Moskowitz and Grinblatt found evidence of macroeconomic industry effects at horizons of one month up to one year, showing that industry effects account for the majority of momentum strategy profits [48]. At even longer horizons of multiple decades, some empirical results have suggested consistent patterns in the impact of business cycles on risk premia [23].

These fundamental and macroeconomic factors are less relevant at short horizons of seconds and minutes. Given the computational challenges of managing high-frequency data and the recency of its rise, it is unsurprising that the high-frequency literature is relatively sparse. Overall, however, results suggest that microstructure factors are the most significant drivers of short-term returns. In 2009, Cao et al. found that limit-order books, beyond the best bid and ask, contain informative value in short-term asset valuation of Australian stocks [14]. They find that supply and demand imbalances in the order book are predictive of future 5-minute returns. Huang and Stoll reached similar conclusions in an emprical analysis of US stocks [34].

These distinctions in market returns across horizons have led to specialization in the marketplace. From an evolutionary perspective, only the players whose skills are best adapted to manage risks and predict returns over a particular horizon can profitably survive and operate at that horizon. The process of specialization might be partially driven by a self-fulfilling prophecy. When an actor adopts a style of trading on a specific horizon, his activity contributes to market behavior and reinforces the relevance of the factors that characterize his strategies. This process can occur regardless of whether the actor's beliefs were correct in the first place. Over time,

when many market participants reach general agreement on the allocation of factors to specific horizons, the true relevance of those factors stabilize, and only the most well-adapted actors at any horizon can sustain profits. This facilitates a permanent specalization of market players into specific niches.

The previous paragraph outlines an interactive dynamic between market returns and market players: the players are subject to the behavior of returns in terms of risks and profits, while returns are inherently driven by the players. Therefore, when studying horizon-specific market characteristics, it is helpful to not only study returns but also understand the processes through which different market participants make decisions. We next discuss how different investment horizons involve sharply different decision-making processes.

In many ways, long-term and short-term investing are fundamentally different problems. The underlying reason for these differences is that historical data can be more effectively leveraged for short-term price predictions. Consider a HFT group that is interested in the 1s horizon. Suppose the group chooses to compile data over a six-month period ($\approx$125 days), a time frame over which it might be reasonable to assume stationarity in microstructure dynamics. This generates approximately 1.9×10^7 relatively independent data points per asset, enabling the development of complex models rich enough to capture sophisticated dynamics. The ability to develop effective models leads many short-term players to pursue data-driven techniques.

On the other hand, at longer investment horizons it becomes infeasible to rely solely on historical data. Imagine a hedge fund that is interested in the annual horizon. Even with decades of historical cross-sectional data across similar assets, it would be difficult to compile more than a few thousand independent data points. Furthermore, the complex macroeconomic landscape that drives annual returns exhibits drastic changes over time. Only the most recent of the few thousand data points are likely to be relevant – imagine the hopeless task of predicting post-2008 macroeconomic trends with only pre-2008 data. With only a handful of data points to model an intricate macroeconomic universe, it is easy to see why purely model-driven approaches have yet to dominate the long-horizon niche. Instead, human market intuition drives the

decision-making at many long-horizon hedge funds.

These differences in trading styles along different investment horizons reinforce the natural differences in returns behavior. The recent surge of high-frequency trading has greatly expanded the spectrum of relevant time horizons, and today the distinctions between longest-horizon and shortest-horizon characteristics are sharper than ever. Despite trading in the same markets, the businesses of fundamental investors like Berkshire Hathaway and high-frequency traders like Virtu Financial exhibit very few similarities. Not only do the two firms serve different roles in the market, but also they are subject to separate regulatory constraints, highly unrelated market risks, and distinct operational logistics. The development of techniques for studying horizon-specific characteristics in the financial markets is now more important than ever.

One potentially useful tool is spectral analysis, also known as frequency domain analysis. We can use the Fourier Transform to decompose a time-domain signal, e.g. a time series of stock returns, into a sum of sinusoids characterized by different frequencies. Each sinusoid in the decomposition reflects the contribution to the signal from the time horizon associated with the cycle length. Analysis of financial dynamics in terms of these sinusoidal cycles leads to natural interpretations in terms of horizon-specific characteristics. For example, long-term dynamics like economic factors and fundamental investing can be captured with low-frequency sinusoids, while short-term dynamics like microstructure effects and high-frequency trading can be captured with high-frequency sinusoids. By decomposing market dynamics into different frequencies, we might gain insight into frequency-specific market changes driven by particular participants and frequency-specific risks associated with operating on particular time horizons. Before we present these spectral techniques in Chapter 2, we first conduct a literature review of spectral analysis in finance.

1.2 Review of Spectral Analysis in Finance

The history of spectral analysis in finance spans many decades [27]. Its origins can be traced to as early as the 1920's, when Beveridge studied cyclical behavior in a

number of settings, from metereological patterns to British export volumes to wheat prices [9] [10]. He found evidence that rainfall data and wheat prices exhibit cycles at similar lengths and theorized about a cause-effect relationship between the two.

The application of spectral analysis to finance was not formally established until a few decades later in 1964, when Granger and Hatanaka published a comprehensive overview of Fourier methods for economic analysis [28]. They established a foundation for modern-day spectral analysis that others have since built upon. For example, the frequency-specific correlation, a quantity that we work with heavily in this paper, was introduced by Croux et al. in 2001 [18].

Because a spectral framework provides a natural representation of cyclic dynamics, it is unsurprising that cycle detection (business cycles in particular) is among the most popular applications of these techniques [27]. In 1999, Baxter and King proposed a band-pass filter for the measurement of business cycles [7]. The key insight is that a band-pass filter allows us to focus on cyclic dynamics along the specific horizons that are relevant to the measurement, defined to range from 1.5 to 8 years in the original paper. The band-pass filter was introduced as an alternative to popular time domain methods like the Hodrick-Prescott filter, which frames cycle detection as an optimization problem [33]. The band-pass filter overcomes two main weaknesses of the Hodrick-Prescott filter: (1) undesired boundary effects and (2) heavy dependence on relatively unintuitive parameters that must be manually selected [7].

Another important area of research the development of regression methods. Because regression is a central tool for economists, the introduction of spectral methods was quickly followed by the expansion of regression analysis from the time domain to the frequency domain. In 1963, Hannan derived spectral properties of ordinary least squares regression and extended the application of generalized least squares regression to the frequency domain [31]. Later in 1974, Engle developed the band spectrum regression (BSR), which focuses regressions to specific frequencies (i.e. specific cycle lengths) [22]. The BSR provides a few potential advantages. First, the effects of noise or data errors can sometimes be more significant along some horizons than others. The BSR allows us to limit the regression to frequencies with higher signal-to-noise

ratios. Second, the BSR enables us to build horizon-specific models with the same data. For example, we could build a short-term model by focusing on high frequencies, and we could build a long-term model by focusing on low frequencies.

We conclude this section with a summary of emprirical results. In 1963, Granger and Morgenstern studied the frequency domain properties of monthly NYSE stock returns, and they found that long-cycle dynamics tend to be stronger than short-cycle dynamics [29]. Over the next few years, Granger observed this pattern so frequently that he named it the "typical spectral shape" in 1966 [26]. Recently in 2015, Chaudhuri and Lo confirmed that this pattern persisted for many decades. However, they discovered that short-cycle dynamics became increasingly more significant with the advent of electronic trading [15]. They analyzed daily returns of NASDAQ/NYSE/AMEX stocks and found that by the 1990s, returns exhibited the most activity at relatively shorter cycles of a only few days. In 1993, Hasbrouck and Sofianos used daily inventories of NYSE market makers to estimate their profits [32]. Using a frequency decomposition of their estimated profits, they determined that the estimated market making profits can be mostly attributed to high frequencies (short investment horizons). These results are intuitive, because market makers profit from short-term price reversals.

1.3 Contrarian Trading Strategies

One way to study the behavior of market participants is to simply mimic them. Although financial firms are secretive about their trading habits, we can simulate their strategies and analyze the implications of the results. Given the proper selection of a representative strategy, we can plausibly capture many real dynamics. Contrarian strategies are one such choice.

Contrarian trading strategies are a class of strategies that involve the buying of recently underperforming assets and the selling of recently overperforming assets. In this paper we define a specific set of strategies that resemble the contrarian strategy first proposed by Lo and MacKinlay [44]. We study the empirical performance of

these strategies later in Chapters 4 and 5.

Consider a universe of N assets, e.g. a collection of securities. At every timestep t, our contrarian strategy is characterized by the weights of a portfolio containing the N assets. Let $w_i[t]$ denote the portfolio weight of the i-th asset at timestep t.

Additionally, let $R_i[t]$ denote the return of the i-th asset over timestep t, and let $R_i[t-T:t-1]$ denote the cumulative return over the timesteps $t-T, t-T+1, ..., t-1$. Then $w_i[t]$ is defined as follows:

$$w_i[t] = R_m[t-T:t-1] - R_i[t-T:t-1], \tag{1.1}$$

$$R_m[t-T:t-1] = \frac{1}{N}\sum_{i=1}^{N} R_i[t-T:t-1]. \tag{1.2}$$

$R_m[t-T:t-1]$ is the mean cumulative return across all N assets. The more the i-th asset overperforms (underperforms) the mean return over the past T timesteps, the more we short (long) it. This strategy is "contrarian" in the sense that it bets on a reversal of recent market trends.

Observe that by the construction of the portfolio weights $w_i[t]$, our contrarian strategy exhibits zero net market exposure: $\sum_{i=1}^{N} w_i[t] = 0$. Market-neutral strategies are ideal for academic studies, because the effects of market drift can often complicate the analysis of performance.

To analyze the performance of our contrarian strategy, we must establish a meaningful measure of strategy returns. The weights $w_i[t]$ can be scaled arbitrarily, scaling the returns as well. In practice, the strategy requires capital to support its positions $w_i[t]$. The ratio of the returns to the amount of required capital provides a normalized measure of strategy performance. If we assume no leveraging, then the buying or selling of \$V's worth of assets requires \$V of capital. Then the unleveraged return on capital, $r[t]$, of our strategy over timestep t is as given in Equation 1.3. Leveraging introduces a multiplicative factor on $r[t]$.

$$r[t] = \frac{\sum_{i=1}^{N} w_i[t]R_i[t]}{\sum_{i=1}^{N} |w_i[t]|} \tag{1.3}$$

In the framework of our contrarian strategy, T represents the time horizon upon which we identify underperformers and overperformers. The weights $w_i[t]$ fluctuate quickly when T is small, producing high-frequency activity in the frequency domain. When T is large, the weights $w_i[t]$ exhibit slower fluctuations, producing more low-frequency activity. By studying this contrarian strategy across a spectrum of T values, we might gain insight into the behaviors of market participants operating at a range of time horizons, from high-frequency traders to longer-horizon quantitative funds. In this paper we study the behaviors of the contrarian strategies parameterized by $T =$ 1 second, 10 seconds, 1 minute, 10 minutes, and 1 hour. We refer to these strategies as the 1s contrarian strategy, the 10s contrarian strategy, the 1m contrarian strategy, etc. In general, we refer to the contrarian strategy with a specific T value as the T-horizon contrarian strategy.

Contrarian strategies are relatively well-studied in the literature [4] [17] [30] [36] [40]. In 1990, Lo and MacKinlay [44] established that the profits of contrarian strategies can be decomposed into two main components. First, the strategy profits from market overreactions, when individual asset returns exhibit negative autocovariance. Second, contrarian strategies profit from the presence of strong lead-lag relationships, when the assets exhibit positive cross-covariance. Both of these components are captured by the systematic buying (selling) of underperformers (overperformers) across a universe of assets.

1.4 Data

In this paper, we work with US equities data over the years 1995-2014. We utilize the following three sources of data, all accessed via the Wharton Research Data Services (WRDS).

1. **The NYSE Trade and Quote (TAQ)** database, which contains intraday trades and quotes data from 1993 to 2014 for all securities listed on the New York Stock Exchange (NYSE), the American Stock Exchange (AMEX), the NASDAQ National Market System (NMS), and the NASDAQ SmallCap Market.

2. **The Center for Research in Security Prices (CRSP)** database, which contains a wide range of information about US securities from 1925 to 2015.

3. **The Standard & Poor's Compustat** databse, which contains company fundamentals and index information.

We use the TAQ database to compute intraday stock returns. From the TAQ quote data, we obtain the National Best Bid and Offer (NBBO) and compute midpoint prices sampled per-second. In this paper, we work solely with midpoint prices instead of trade prices. This avoids spurious dynamics introduced by sampled trade prices, such as the bid-ask bounce [47] and effects of nonsynchronous trading [43]. We compute per-second arithmetic returns from these mid point prices. We ignore overnight returns and assume that the first second after the market open immediately succeeds the last second before the previous close.

The TAQ database contains only raw prices that are not adjusted for dividends, mergers, stock splits, etc. Our analysis is generally unaffected by these events, because we strictly work with intraday returns.

From the CRSP database, we retrieve the Standard Industrial Classification (SIC) codes of all relevant stocks. The SIC classification system maps industries to a four-digit code. We use the SIC codes of stocks to construct sector portfolios in Section 3.2.

Finally, from the S&P Compustat database we obtain the historical constituents of the S&P 500, S&P MidCap 400, and S&P SmallCap 600 indices. We use the constituents to construct market capitalization portfolios in Section 3.2. Additionally, in Chapters 4 and 5 we simulate contrarian trading strategies over the constituents of the S&P Composite 1500 Index, a union of the three indices above.

As in most studies, our dataset is not perfect. We discuss the management of data issues in Appendix A.

Chapter 2

Spectral Analysis Techniques

Spectral analysis involves the transformation of a time domain signal into the frequency domain. Intuitively, this transformation is a decomposition of a time series into a sum of periodic functions. In this paper we focus on Fourier analysis techniques, in which the periodic functions are sinusoids. In this framework, a time series is viewed as a linear combination of sinusoids of different frequencies. Other functions, such as wavelets, can be applied as well, and we briefly discuss their potential advantages in Section 2.3.2.

We focus on discrete time techniques, because our applications, like most financial applications, involve sampled data (e.g. stock returns sampled per second). We do not explicity present the corresponding continuous time results, which are analogous.

The representation of a time series in the frequency domain can be useful when operations on the periodic components are interpretable. In financial applications, the component of a time series attributed to the sinusoid of frequency Ω radians/sample can be interpreted as activity at the specific horizon associated with Ω. This horizon is the full cycle length of the sinusoid, $2\pi/\Omega$ samples or $2\pi T_s/\Omega$ time units, where T_s is the sampling period. With this in mind, the analysis of financial dynamics in the frequency domain can be directly construed in terms of horizon-specific behavior. Below we present our techniques. We aim for an intuitive discussion that helps orient the reader to financial applications.

2.1 Discrete Fourier Transform

The Discrete Fourier Transform (DFT) is the basic building block of our spectral analysis techniques. It defines the decomposition of a time-domain signal into the frequency domain. The DFT can be efficiently computed with the Fast Fourier Transform (FFT) algorithm.

Definition 2.1.1. *Consider a discrete-time signal $x[n]$ of finite length N. The Discrete Fourier Transform $X[k]$ of $x[n]$ is defined as follows for $k = 0, 1, ..., N-1$.*

$$X[k] = \sum_{n=0}^{N-1} x[n] e^{-j\Omega_k n}, \text{ where } \Omega_k = \frac{2\pi k}{N} \tag{2.1}$$

Intuitively, $X[k]$ can be seen as the dot product between $x[n]$ and the complex exponential of frequency Ω_k. The dot product between two vectors $\mathbf{a}$,$\mathbf{b}$ is associated with their cosine similarity: $\mathbf{a} \cdot \mathbf{b} = \|\mathbf{a}\| \|\mathbf{b}\| \cos(\theta)$. For fixed $\|\mathbf{a}\|$ and $\|\mathbf{b}\|$, a large dot product indicates a small angle between the two vectors, while a dot product near zero indicates that the two vectors are orthogonal. In this light, $X[k]$ is the degree to which $x[n]$ aligns with the sinusoid of frequency Ω_k. Expressed more concisely, $X[k]$ describes the activity of $x[n]$ at frequency Ω_k. Specifically, $|X[k]|$ measures the strength of the activity, while $\angle X[k]$ measures the phase shift. The quantity $|X[k]|^2$ is often interpreted as the power of $x[n]$ at frequency Ω_k. The values of $X[k]$ are called the DFT coefficients of $x[n]$, a name inspired by the following property.

Theorem 2.1.2. *A discrete-time signal $x[n]$ of finite length N can be reconstructed from its DFT coefficients $X[k]$ through the following Inverse Discrete Fourier Transform.*

$$x[n] = \frac{1}{N} \sum_{k=0}^{N-1} X[k] e^{j\Omega_k n}, \text{ where } \Omega_k = \frac{2\pi k}{N} \tag{2.2}$$

Equation 2.2 states the values of $X[k]$ are simply the coefficients of $x[n]$ expressed in the basis of complex exponentials (up to a scaling factor of $1/N$). This is consistent with the notion that the DFT is a basis transform. Additionally, we note that $X[k]$ is conjugate symmetric about $N/2$: $X[k] = \overline{X}[N-k]$ for $k = 1, 2, ..., N/2$, for which

we provide a brief explanation: Because the frequency Ω is periodic with $e^{j\Omega_k n} = e^{j(\Omega_k - 2\pi)n}$, for $k = 1, 2, ...N/2$ we have that

$$e^{j\Omega_k n} = \overline{e^{-j\Omega_k n}} = \overline{e^{j(2\pi - \Omega_k)n}} = \overline{e^{j\Omega_{N-k} n}}.$$

The conjugate symmetry about $k = N/2$ follows and directly leads to the property that $|X[k]| = |X[N-k]|$ for $k > 0$. As a result, $X[k]$ and $X[N-k]$ are associated with the same frequency. Understanding the conjugate symmetry of the DFT coefficients is essential for the proper interpretation of the techniques in this section and in Section 2.2.

We conclude this section with a simple example. In Example 1, we illustrate how the DFT can sometimes provide valuable insight that is not obvious in the time domain.

Example 1. *Consider a time series* $x[n] = 2\sin\left(\frac{2\pi\times 40}{100}n - 5\right) + 2\cos\left(\frac{2\pi\times 25}{100}n + 30\right) + \epsilon_n$ *for* $n = 0, 1, ..., 99$*, where* $\epsilon_n \sim N(\mu = 0, \sigma^2 = 1)$*. Figure 2-1 plots* $x[n]$ *and* $|X[k]|$*.*

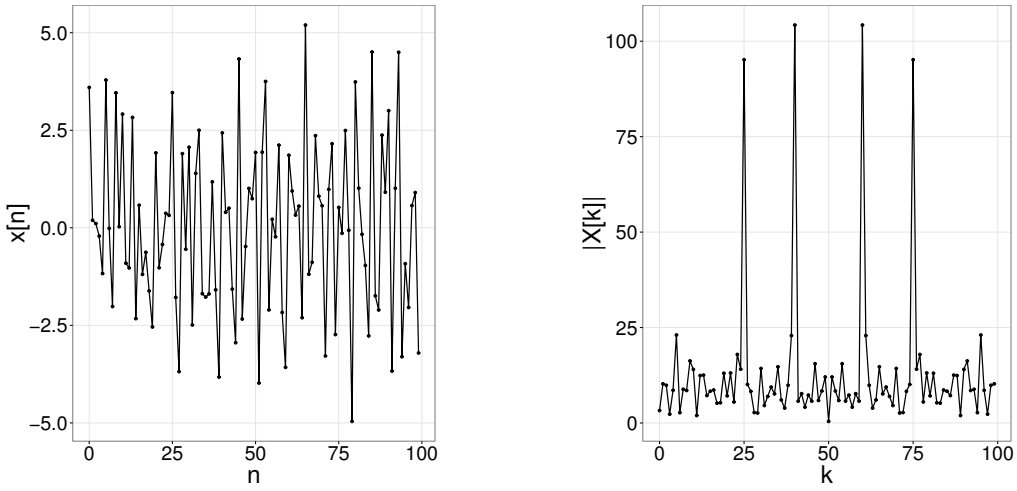

(a) $x[n]$ (b) $|X[k]|$

Figure 2-1: A realization $x[n]$ of our random process and the magnitudes of its corresponding DFT coefficients, $|X[k]|$.

We observe two pairs of peaks in $X[k]$ at frequencies corresponding to the two periodic components of $x[n]$. In this example, the strong underlying trends are not

obvious from the time domain perspective in Figure 2-1a. Without considering the frequency domain representation in Figure 2-1b, one might mistakenly conclude that $x[n]$ is "random" noise.

2.2 Frequency Decomposition via Parseval's Theorem

The Discrete Fourier Transform is useful, but it only allows us to study a single time series. In this section we present a version of Parseval's Theorem, which allows us to decompose the realized cross-moment of two time series across frequencies. Parseval's Theorem, stated next, is particularly useful because cross-moments can represent relatively sophisticated dynamics, such as asset correlations and the performance of trading strategies.

Theorem 2.2.1. *Suppose that $x[n]$ and $y[n]$ are two finite, real-valued discrete-time signals of length N, and let $X[k]$ and $Y[k]$ denote their respective DFT coefficients. Then the following equality holds.*

$$\frac{1}{N}\sum_{n=0}^{N-1} x[n]y[n] = \frac{1}{N^2}\sum_{k=0}^{N-1} X[k]\overline{Y}[k], \text{ where } \overline{Y}[k] \text{ is the complex conjugate} \tag{2.3}$$

Parseval's Theorem states that the dot product of two signals can be equivalently computed in the time domain and in the frequency domain, up to a scaling factor of $1/N$. The right-hand side of Equation 2.3 can be intuitively interpreted in the frequency domain. Each term indicates the degree to which $x[n]$ and $y[n]$ move together at a specific frequency. Parseval's Theorem leads us to conclude that the realized cross-moment of any two time domain signals can be decomposed into alignments across individual frequencies.

Recall from Section 2.1 that the DFT coefficients are conjugate symmetric about $k = N/2$. As a result, the imaginary parts of $X[k]\overline{Y}[k]$ and $X[N-k]\overline{Y}[N-k]$ cancel in Equation 2.3, implying that the they make identical real contributions to the realized

cross-moment. For these two reasons, we assign the intepretation of k and $N-k$ to the same frequency. The contribution of the highest-frequency components correspond to values of k closest to $N/2$, and the lowest-frequency components correspond to values of k closest to 0 and $N-1$. Specifically, $X[k]$ can be associated with activity at a time horizon of $2\pi T_s/\Omega_k = NT_s/k$ for $k = 1, 2, ..., N/2$, where T_s is the sampling period. The value $k = 0$ corresponds to an infinite horizon.

In the next two sections we discuss applications of Parseval's Theorem in a financial context. When $x[n]$ and $y[n]$ are two time series of returns, the cross-moment is the covariance plus a DC (zero-frequency) component. When $x[n]$ is a time series of trading strategy weights and $y[n]$ is a time series of returns, the cross-moment is the performance (return) of the strategy.

2.2.1 Covariance and Correlation

Consider two length-N time series of returns, $r_1[n]$ and $r_2[n]$, with corresponding DFT coefficients $R_1[k]$ and $R_2[k]$. Then a direct application of Equation 2.3 produces the frequency decomposition of the realized cross-moment in Equation 2.4.

$$\frac{1}{N}\sum_{n=0}^{N-1} r_1[n]r_2[n] = \frac{1}{N^2}\sum_{k=0}^{N-1} R_1[k]\overline{R_2}[k] \tag{2.4}$$

Substracting the zero-frequency component from both sides of Equation 2.4 gives a frequency decomposition of the sample covariance in Equation 2.5. Depending on the context, the realized cross-moment is sometimes preferred over the sample covariance as a covariance estimate, when the population means are known to be zero. When $r_1[n] = r_2[n]$, we have a frequency decomposition of the second moment or variance.

$$\hat{\text{cov}}(r_1, r_2) = \frac{1}{N^2}\sum_{k=1}^{N-1} R_1[k]\overline{R_2}[k] \tag{2.5}$$

Each term in the right-hand sides of Equations 2.4 and 2.5 reflect the degree to which $r_1[n]$ and $r_2[n]$ move together along a specific frequency. This frequency decomposition allows us to estimate covariance along a particular set of frequencies K

by simply summing the individual contributions, shown in Equation 2.6. Intutively, this is equivalent to partially reconstructing $r_1[n]$ and $r_2[n]$ using a subset of frequencies (i.e. subset of the DFT coefficients) and computing the covariance of the reconstructed returns. We note that K must contain symmetric pairs of k values to be meaningful (see Section 2.1). Equation 2.6 allows us to construct covariance estimates across specific frequency bands.

$$\text{cov}_K(r_1, r_2) = \frac{1}{N^2} \sum_{k \in K} R_1[k]\overline{R_2}[k] \tag{2.6}$$

The notion of frequency-specific covariance leads to frequency-specific correlation in Equation 2.7. The frequency-specific correlation, like the traditional correlation, ranges from -1 to 1 and can be interpreted in the same manner. It is equivalent to the time-domain correlation of the partially reconstructed signals.

$$\text{corr}_K(r_1, r_2) = \frac{\text{cov}_K(r_1, r_2)}{\sqrt{\text{var}_K(r_1)\text{var}_K(r_2)}} \tag{2.7}$$

We might be motivated to calculate frequency-specific covariance and correlation for a number of reasons. For example, it could be that our process of interest is particularly noisy at high frequencies. In such a case, we might be interested in estimating covariance and correlation across the lower frequencies that are less heavily impacted by noise. Another motivation might be an interest in a specific time horizon. With longer investment horizons, we might be indifferent towards cyclical behavior at high frequencies. A frequency-specific analysis would allow us to focus on behavior at the relevant horizon.

2.2.2 Performance of Trading Strategies

As we have seen, the realized cross-moment of any two time series can be decomposed across frequencies via Parseval's Theorem. When one time series is a vector of weights and the other is a vector of asset returns, the cross-moment represents the performance of the trading strategy characterized by the weights. Suppose we have a length-

N time series of an asset's returns, $r[n]$, and a length-N time series of weights, $w[n]$, describing a strategy's exposure to the asset at each period. Then $W[k]$ and $R[k]$ denote their corresponding DFT coefficients, and Parseval's Theorem produces a frequency decomposition of the average per-period trading profits, shown in Equation 2.8.

$$\frac{1}{N}\sum_{n=0}^{N-1} w[n]r[n] = \frac{1}{N^2}\sum_{k=0}^{N-1} W[k]\overline{R}[k] \tag{2.8}$$

Real trading strategies typically involve more than a single asset, and we can extend this framework to an arbitrary number of assets. Suppose our relevant universe consists of M assets, and let $w_i[n]$ and $r_i[n]$ denote the weights and returns of the ith asset. Then the total strategy profits are simply the sum of the profits gained over all M assets, below in Equation 2.9.

$$\frac{1}{N}\sum_{i=1}^{M}\sum_{n=0}^{N-1} w_i[n]r_i[n] = \frac{1}{N^2}\sum_{i=1}^{M}\sum_{k=0}^{N-1} W_i[k]\overline{R_i}[k] = \frac{1}{N^2}\sum_{k=0}^{N-1}\sum_{i=1}^{M} W_i[k]\overline{R_i}[k] \tag{2.9}$$

This decomposition attributes trading profits to distinct frequencies. Each term in the right-hand sides of Equations 2.8 and 2.9 reflects the degree to which the changes in weights align with asset returns at a specific frequency. Thus, the decomposition allows us to evaluate an investor's timing ability at different horizons. As in the covariance discussion in Section 2.2.1, we can study profits over a range of frequencies by summing profits along a frequency band K, as long as K includes symmetric pairs of k. These frequency-band profits are equivalent to calculating the profits from partially reconstructed (with a subset of the DFT coefficents) $w_i[n]$ and $r_i[n]$.

Let us provide a bit of intuition for this frequency decomposition of profits. High frequency traders rapidly adjust portfolio weights at a sub-second level. Therefore, we expect that the majority of their profits can be attributed to high-frequency components. Fundamental hedge funds, on the other hand, adjust weights much less frequently, and we expect that low-frequency components account for the majority

of their profits. A fund that is unable to deliver profits at its relevant frequencies provides little value to its investors.

Chaudhuri and Lo [16] showed that this frequency decomposition of trading profits closely relates to Lo's Active-Passive (AP) decomposition [42]. In the AP decomposition, the passive component is the profit earned by holding the mean weights, and the active component is the remainder. With respect to this frequency decomposition framework, the passive component is the zero frequency ($k = 0$) component of the profit, and the active component is the sum of the nonzero frequencies.

2.3 Practical Challenges in Financial Applications

The application of spectral analysis techniques financial settings is particularly difficult for many reasons. We summarize these challenges into three categories: noise, nonstationarity, and aliasing. We argue that spectral techniques are less vulnerable to aliasing effects than conventional time-domain methods and consequently might be superior.

2.3.1 Noise

The DFT is inherently noisy, and the notoriously low signal-to-noise ratios in financial data exacerbate this weakness. The DFT is noisy in the sense that it is an inconsistent estimator: the DFT coefficients of a realization of a stationary, ergodic random process do not converge to the true spectral content of the process as the number of data points grows. This is because the number of DFT coefficients to estimate grows with the data, and the coefficients are approximately independent. As a result, the number of data points per coefficient does not grow with the data, and the law of large numbers does not apply. A more reliable estimate of the spectral content must involve some form of averaging.

One convenient solution, which we adopt empirically in this paper, is to apply smoothing (local averaging) to the DFT coefficients. The typically preferred smoothing method is the modified Daniell filter, which exhibits relatively less spectral leak-

age [11]. Generally speaking, smoothing implements a classic bias-variance tradeoff, allowing us to reduce wild fluctuations due to noise by sacrificing peak resolution. Although smoothing is simple to apply, a main disadvantage is that selecting a proper degree of smoothing requires intuitive judgement.

Another class of solutions involves the allocation of the time-domain signal into multiple blocks and averaging the DFT coefficients produced across all blocks. The simplest such technique, called Bartlett's method, partitions the time-domain signal into contiguous non-overlapping blocks [6]. In Welch's method, the blocks are contiguous but overlapping, and each partition is preprocessed by applying a window function [59]. This window function is typically center-heavy to reduce spectral leakage. Finally, in the multitaper method, the individual blocks consist of the entire signal applied with different taper functions [56]. Orthogonal taper functions are typically preferred for better estimation quality.

2.3.2 Non-stationarity

The DFT is only meaningful under assumptions of stationarity, because it produces a single estimate for the spectral content of an entire signal. It would be inappropriate to directly apply the DFT to a signal whose true spectral behavior changes over the course of the signal. Unfortunately, financial processes are strongly non-stationary – for example, the rise of electronic trading has undoubtedly transformed the horizon-specific properties of asset returns. Since we are inherently interested in studying changes over time, this dependence on stationarity is a fundamental weakness of the DFT.

The most standard solution to this problem is the short-time Fourier transform (STFT), which we apply in our empirical studies in Chapters 3-5. This method involves the allocation of the time signal into contiguous blocks of equal size and separately estimating the spectral density (e.g. computing the DFT coefficients) of each block. We can infer changes over time from differences in the spectral density across blocks. While simple, the STFT exhibits two main weaknesses.

First, results are heavily dependent on the manually selected block size, which

tunes a trade-off between frequency resolution and time resolution. If block sizes are too large, then we can estimate the behavior at many frequencies but are left with fewer blocks over which to identify temporal changes – we achieve high frequency resolution at the cost of poor time resolution. If block sizes are too small, then vice versa.

A second and perhaps more important weakness is that the STFT generally achieves a suboptimal trade-off between frequency and time resolution. In the STFT, each block is of equal size, meaning that we estimate low-frequency and high-frequency components with the same number of data points. This produces poorer resolution at the low frequencies than if we computed the DFT of the entire signal, because the cycle lengths represented by the DFT coefficients follow a harmonic pattern. Additionally, a robust estimation of long-cycle activity naturally requires more data points. For the measurement of low-frequency activity, we would prefer to allocate our time signal into fewer blocks that are larger.

While long cycles are underrepresented in the DFT coefficients, short cycles are overrepresented. At high frequencies, the STFT achieves extremely fine frequency resolution at the cost of poor time resolution. Compared to lower frequencies, the estimation of high-frequency activity requires fewer data points. For the measurement of high-frequency activity, we would prefer to allocate our signal into many blocks that are smaller, increasing our sensitivity to changes over time.

With the STFT, it is impossible to simultaneously achieve good frequency resolution at low frequencies and good time resolution at high frequencies. This might be possible, however, with wavelet analysis. In a wavelet transform, low-frequency activity is estimated using more data points, and high-frequency activity is estimated using fewer data points [53] [46]. Although this is a signifcant advantage, wavelet analysis also presents the disadvantage of increased complexity. A meaningful analysis requires an appropriate selection of the wavelet shape, and the proper interpretation of wavelet transform results is more involved. A deeper discussion of wavelets is beyond the scope of this paper.

Despite its weaknesses, the STFT remains a popular method of handling non-

stationarity. Its inability to achieve both frequency resolution and time solution might not be critical, because an acceptable trade-off can often be attained through a simple tuning of block size. The simplicity of the STFT provides great flexibility and produces easily intepretable results. At the very least, it might be worthwhile to first establish a rudimentary analysis via the STFT before attempting more sophisticated techniques.

2.3.3 Aliasing

Finally, we discuss aliasing, a relatively unexplored issue in the context of financial analysis. Given a discrete time-sampled signal, the shortest cycles that can be measured are cycles over two data points. In order to properly capture activity across all frequencies, the signal must be sampled quickly enough to detect the highest-frequency activity of the underlying continuous process. Specifically, when this highest frequency in the underlying continuous process is B, the minimum proper sampling rate is $2B$, known as the Nyquist rate. When the signal is sampled below this rate, aliasing occurs, and the uncaptured high-frequency activity in the underlying process becomes misattributed to the frequencies that are captured in the sampled signal. For a deeper discussion of aliasing, we refer the reader to standard signal processing textbooks.

This presents a fundamental challenge for the analysis of recent (and future) financial dynamics. Today, the fastest high-frequency traders transact at the millisecond horizon, some even into microseconds. This implies that to achieve truly alias-free sampling we must sample at the corresponding Nyquist rate. Unfortunately, with present-day technology this granularity is computationally infeasible for studies across long periods of time or wide ranges of assets. The effects of aliasing in finance will become increasingly important to understand as more activity occurs on horizons shorter than we can reasonably sample.

We argue that conventional time-domain methods are particularly vulnerable to these aliasing effects. When studying the behavior of returns along a specific horizon, it is typical to analyze returns sampled at the horizon length. For example, suppose

we are interested in studying daily effects using a year's worth of per-second returns. In the conventional time-domain methods, we cumulate these per-second returns into daily returns and perform analyses with the latter. Despite having access to per-second returns, we essentially operate as if we were only capable of daily sampling. Although intuitive, the daily-sampled returns do not fullly leverage the granularity of our available data. Our daily returns are completely blind to any cyclical activity at horizons shorter than two days (the period corresponding to the Nyquist frequency). Any such activity is aliased and will be misattributed to frequencies associated with horizons of multiple days or more. This aliasing flaw of the conventional horizon-sampling methods will grow in significance as financial processes become increasingly driven by high-frequency activity.

Although some degree of aliasing is generally unavoidable, a spectral framework is less susceptible to its effects. Unlike conventional methods, a spectral approach leverages the full granularity of the available data. Regardless of the horizon we study, we always operate with the finest-sampled data. When studying behaviors at longer horizons, we simply examine longer cycles over more data points. A spectral approach subjects us to the same minimum possible degree of aliasing, regardless of our target horizon. In the example from the previous paragraph, with a spectral approach only cycles shorter than two *seconds* (instead of two *days*) would be aliased.

Chapter 3

Analysis of Returns

In this chapter we apply spectral analysis techniques from Chapter 2 to analyze empirical returns. In our results we perform smoothing of spectral quantities via a series of Daniell filters (see discussion in Section 2.3.1). In Section 3.1 we study the returns of individual stocks, and in Section 3.2 we study the returns of portfolios.

In this paper we present spectral results in a manner that encourages direct interpretation in terms of financial horizons. This might induce a bit of confusion, which we address here. The DFT allows us to study the behavior of a length-N time domain signal at specific frequencies of $\Omega_k = 2\pi k/N$ for $k = 0, 1, ..., N-1$, where values of k symmetric about $N/2$ correspond to the same frequency (see discussion in Section 2.1). In engineering, it is conventional to graph spectral quantities with k along the horizontal axis.

However, for financial applications it is more relevant to consider the cycle length corresponding to the k-th frequency, $T_k = 2\pi/\Omega_k = N/k$, for $k = 1, 2, ..., N/2$. In this paper we choose to diverge from the engineering convention and instead graph spectral quantities with T_k along the horizontal axis. Because of the functional behavior of N/k, we have many frequencies corresponding to shorter cycles and few frequencies corresponding to longer cycles.

This might introduce some minor confusion when examining graphs of quantities like normalized variance, in which the sum over all frequencies must be 1. The sum over all frequencies is difficult to visually verify when the horizontal axis is T_k instead

of k. Despite this inconvenience, we believe it is more valuable to present spectral results in a financially interpretable manner.

3.1 Individual Stock Returns

Here we demonstrate how our spectral tools can be used to study the behavior of individual stock returns. We apply a frequency decomposition of variance and calculate frequency-specific correlations. We refer to a set of correlation coefficients across a range of frequencies as a correlation spectrum.

3.1.1 Frequency Decomposition of Variance

Using Equation 2.5 we can perform a frequency decomposition of the variance of a series of per-second returns. Figure 3-1 illustrates the frequency decomposition of variance in Microsoft Corp. (MSFT) returns over the past 2 decades. It shows the fraction of total variance that can be attributed to cycles of various frequencies.

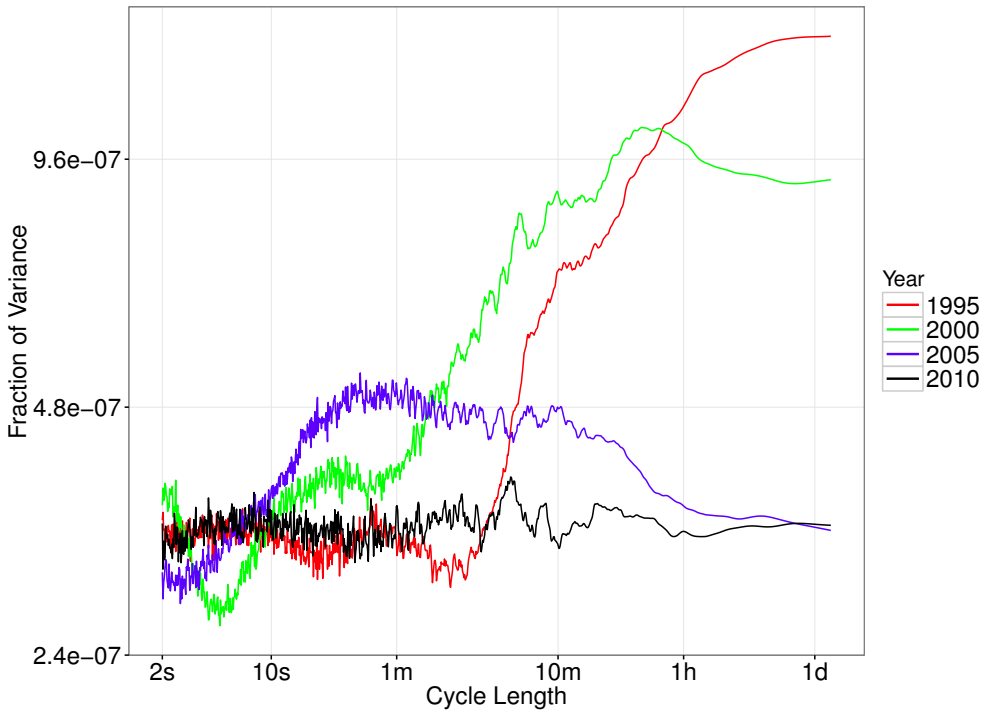

Figure 3-1: Smoothed frequency decomposition of variance in annual per-second returns of Microsoft stock across the years 1995-2010.

As we progress in time from 1995 to 2010, we see a consistent trend in the variance decomposition – an increase in the fraction of variance that is attributed to shorter cycles. The cycle lengths that account for the highest fraction of the variance shrinks from 1d (1995) to ≈30m (2000) to ≈30s (2005). By 2010, we see that the frequency decomposition of the variance is virtually flat.

This shift in the variance decomposition reflects the steady rise of electronic trading. Short-horizon market players trade frequently and account for a large portion of total trade volume. As a result, their behaviors significantly drive the dynamics of returns. The years 1995-2010 witnessed a massive reduction in the trading horizons of electronic market makers, and Figure 3-1 captures the growth in high-frequency activity that they produced. Because our returns data are sampled at 1s intervals, the shortest cycles visible to us are of length 2s. If our data were sampled at extremely fine intervals, with this technique we could possibly visualize the push by high-frequency traders into the millisecond horizon.

3.1.2 Correlation Spectrum

Next, by applying Equation 2.7 we can calculate frequency-specific correlations, the degree to which two stocks move together along specific frequencies. Below we compare the behaviors of two pairs of stocks and identify differences between the two correlation spectra. One pair is The Coca-Cola Co. (KO) and PepsiCo Inc. (PEP), while the other pair is Exxon Mobil Corp. (XOM) and Southwest Airlines Co. (LUV).

We intuitively expect differences between the two pairs. On the one hand, Coca-Cola and PepsiCo are extremely similar businesses that share many types of market exposures. We expect the two stocks to move closely together, especially along longer cycles at which fundamentally driven factors operate. On the other hand, Exxon and Southwest share relatively few long-term economic factors. In fact, Exxon is positively exposed to oil while Southwest is negatively exposed. Although we expect both to move with short-term buying and selling pressures in the general market, we might not expect them to move closely over longer cycles.

Figure 3-2 graphs the correlation spectra over the years 2000-2012. We see that

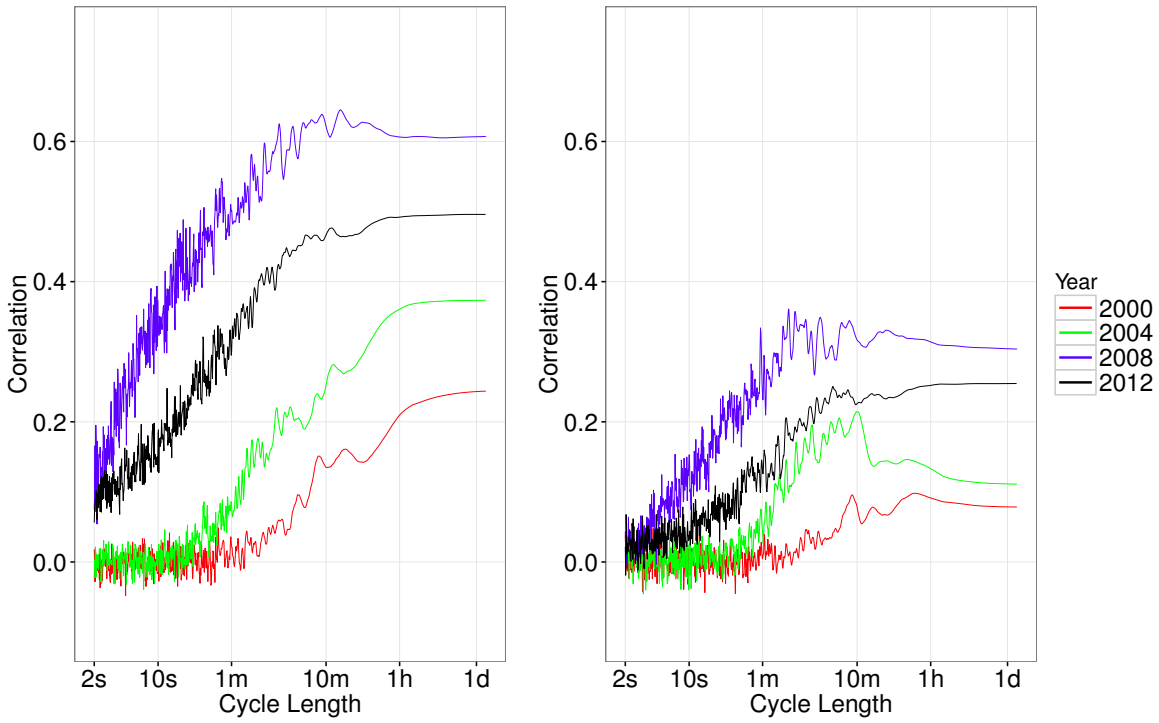

(a) Coca-Cola and PepsiCo

(b) Exxon Mobil and Southwest Airlines

Figure 3-2: Smoothed correlation spectra between annual per-second returns of (a) Coca-Cola and PepsiCo and between (b) Exxon Mobil and Southwest Airlines across the years 2000-2012.

the graphs are generally consistent with our intuition. Throughout the years, we first confirm that Coca-Cola and PepsiCo move more closely together than Exxon and Southwest at all frequencies. More interestingly, we highlight differences in curve shape between Figures 3-2a and 3-2b. The Coca-Cola and PepsiCo curves in Figure 3-2a maintain positive slopes over longer cycle lengths. In 2000, the peak correlation between Coca-Cola and PepsiCo occurs at 1d cycles, while peak between Exxon and Southwest occurs at cycles of length 10m-1h. In 2004, the Coca-Cola and PepsiCo curve peaks at 1h-1d, while the Exxon and Southwest curve peaks at ≈10m. In 2008, the Coca-Cola and PepsiCo peak occurs at ≈10m, while the Exxon and Southwest peak occurs at ≈2m. Finally in 2012, the Coca-Cola and PepsiCo curve peaks at 1h-1d, while the Exxon and Southwest curve arguably peaks at 10m-1d. The years 2013 and 2014, not shown, are similar to 2012. These observations are consistent with our intuition that Coca-Cola and PepsiCo are driven by shared economic factors,

while Exxon and Southwest are not. Because economic factors are more relevant over longer cycles, we expect Coca-Cola and PepsiCo to exhibit maximum correlation at longer cycles than Exxon and Southwest. Overall, we conclude that the shape of the correlation spectrum is determined by the types of shared exposures.

We also discover that the relevance of fundamental economic factors at shorter horizons has grown immensely. In 2000 and 2004, the correlations between the two pairs of stocks are nearly identical at cycles of lengths up to 10m. However, in 2008 and 2012 we see that Coca-Cola and PepsiCo exhibit noticeably higher correlation than the other pair, even at cycles of length 2s. This implies that fundamental economic factors were completely irrelevant at short horizons only a decade ago, but they are very much relevant today. This change might be possibly due to a self-fullfilling prophecy driven by high-frequency traders.

3.2 Portfolio Returns

In this section, we extend our analysis of individual stocks to portfolios. First, we construct the following equal-weighted market capitalization portfolios.

- LARGE Portfolio: Equal-weighted portfolio of **S&P 500** stocks
- MID Portfolio: Equal-weighted portfolio of **S&P MidCap 400** stocks
- SMALL Portfolio: Equal-weighted portfolio of **S&P SmallCap 600** stocks

In addition, we construct equal-weighted sector portfolios. Each portfolio consists of a subset of the stocks in the **S&P 500** Index. The allocation of stocks to sectors is determined by the Standard Industrial Classifcation (SIC) code of each stock, described in Appendix B. We formulate the following equal-weighted sector portfolios.

- CNSMR (Consumer) Portfolio
- MANUF (Manufacturing) Portfolio
- TECH (Technology) Portfolio

- HEALTH Portfolio
- FINANCE Portfolio

3.2.1 Frequency Decomposition of Variance

As shown for MSFT returns in Figure 3-1, we confirm that the variance of general market also exhibits a steady expansion into higher frequencies. Figure 3-3 graphs the frequency decomposition of variance of the LARGE portfolio. We see that as we progress in time, the shorter cycles become increasingly relevant. In 1995, cycles of lengths at least 3m account for a abnormally (compared to white noise) large portion of the total variance. In 2000, this length shrinks to ≈1.5m, and in 2005 it shrinks even further to ≈30s. By 2010, the variance is so evenly distributed across frequencies that the curve is almost flat. This frequency decomposition of variance illustrates the push into shorter horizons driven by high-frequency trading.

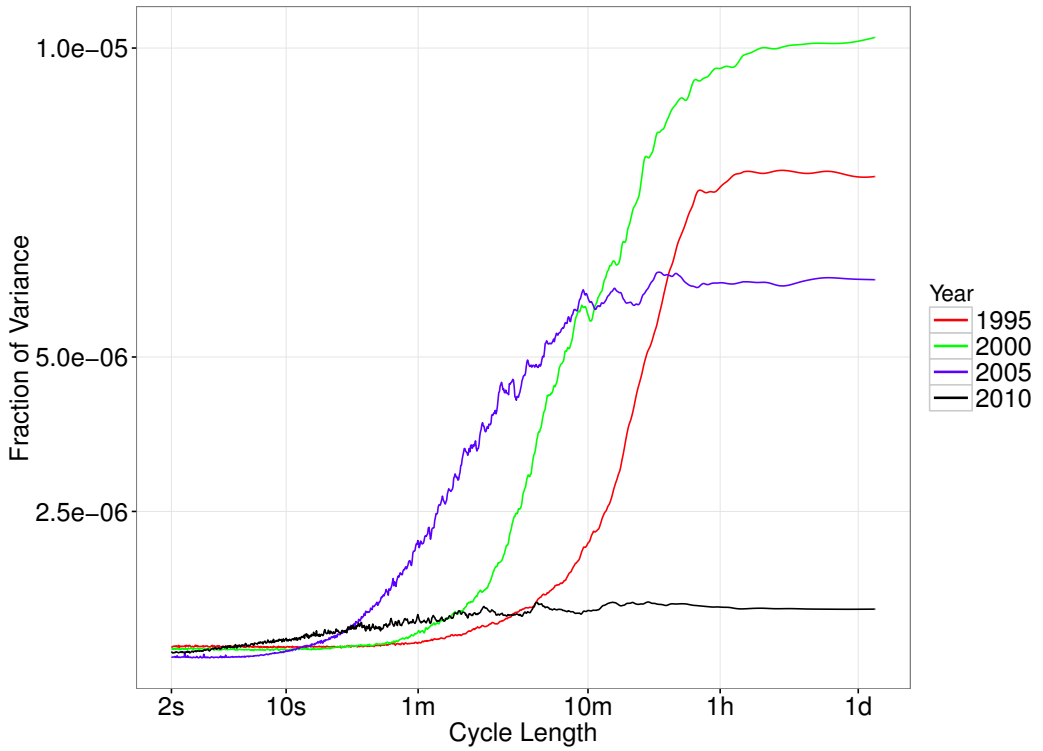

Figure 3-3: Smoothed frequency decomposition of variance in annual per-second returns of the equal-weighted large-cap portfolio (containing S&P 500 constituents) across the years 1995-2010.

3.2.2 Correlation Spectrum

Next, we study the behavior of the correlation spectrum for pairs of cap portfolios and pairs of sector portfolios.

Market Cap Portfolios

We compare the correlation spectrum between the LARGE and MID portfolios and the spectrum between the LARGE and SMALL portfolios. This comparison illustrates the role of market capitalization in determining spectral properties.

Figure 3-4 plots the two correlation spectra over the years 2000-2012. We generally see that across all years and all frequencies, the LARGE-MID correlation is higher than the LARGE-SMALL correlation. This result confirms the intuition that market cap affects the type of factors that a stock is exposed to. For example, larger companies are typically more strongly associated with macroeconomic factors, such as the general health of the U.S. economy. Therefore in general, with this intuition we expect stocks with similar market capitalizations to behave more similarly than otherwise.

Furthermore, we find that the curves are monotonic nondecreasing functions of cycle length. The larger the cycle length, the more closely MID and SMALL move with LARGE. This suggests that the LARGE, MID, and SMALL portfolios are driven by extremely similar long-term factors but relatively distinct short-term factors.

Finally, we highlight the differences in curve shape between LARGE-MID and LARGE-SMALL. The LARGE-MID curves in Figure 3-4a generally approach their 1d-cycle correlations more quickly than the LARGE-SMALL curves in Figure 3-4b. For example, consider the correlation at 10m-cycles in 2000. LARGE-MID exhibits over 2/3 of its 1d correlation, while LARGE-SMALL exhibits less than 1/2 of its 1d correlation. Similarly, consider 1m-cycles in 2003. LARGE-MID exhibits 2/3 of its 1d correlation, while LARGE-SMALL exhibits less than 1/2. This pattern persists in 2006, 2009, and 2012 as well.

The shorter the cycle length, the greater the difference between the LARGE-MID

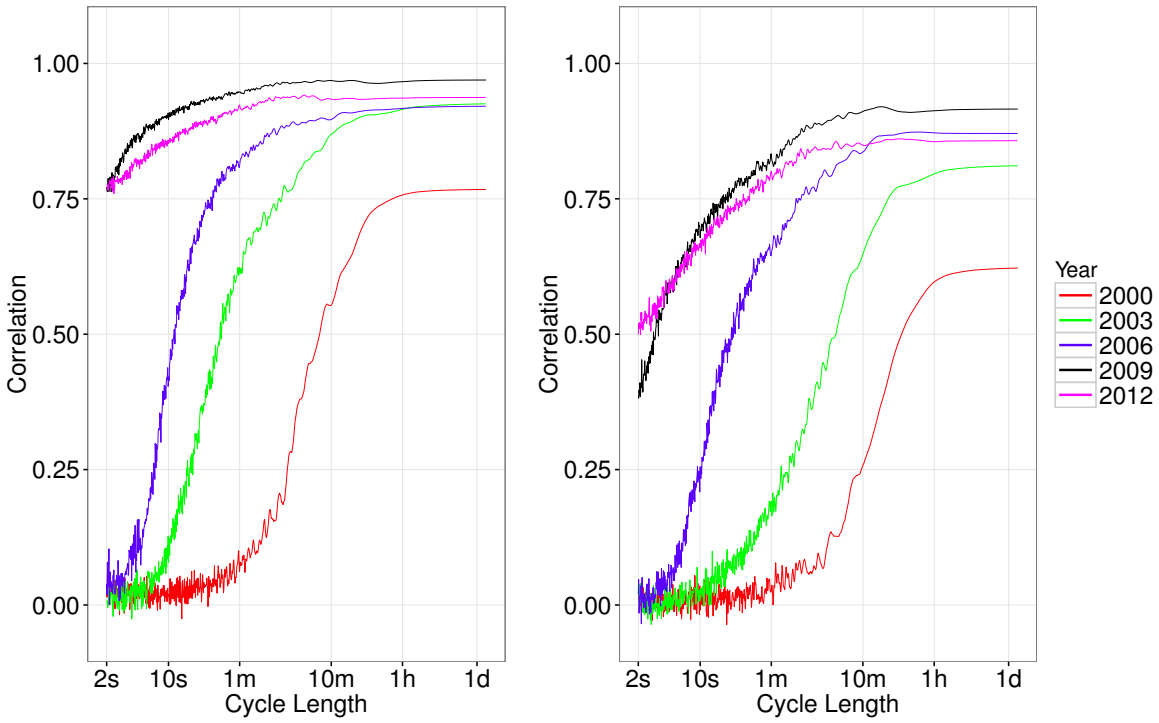

(a) Large-cap and mid-cap

(b) Large-cap and small-cap

Figure 3-4: Smoothed correlation spectra between annual per-second returns of equal-weighted market capitalization portfolios across the years 2000-2012. The spectrum between the large-cap portfolio (containing S&P 500 constituents) and the mid-cap portfolio (containing S&P 400 constitutents) is shown in (a), while the spectrum between the large-cap portfolio and the small-cap portfolio (containing S&P 600 constitutents) is shown in (b).

and LARGE-SMALL correlations. A possible explanation is that liquidity becomes increasingly important at shorter horizons. First, illiquid stocks trade less and experience fewer quote updates. As a result, an illiquid stock might exhibit minimal short-cycle actvity simply because its midpoint rarely moves at that horizon. Secondly, liquid and illiquid stocks attract different types of market participants. Some market players that specialize in short horizons, such as high-frequency market makers, mostly trade in relatively liquid markets. As a result, any short-term behaviors that these participants generate would then only appear in liquid stocks. According to this explanation, MID behaves more similarly to LARGE than SMALL along short cycles solely because MID stocks are more similar to LARGE stocks in terms of liquidity. MID and SMALL both move closely with LARGE along longer cycles,

because liquidity factors ares less relevant at longer horizons.

Sector Portfolios

Finally, we study the relationships between our five equal-weighted sector portfolios (CNSMR, MANUF, TECH, HEALTH, FINANCE) and examine how these relationships have changed across horizon and across time. In Figure 3-5, we graph the correlation spectra between TECH and the other four sector portfolios across 2000-2014.

The most distinctive feature is the surge in short-cycle connectedness between 2006 and 2010. The sector correlations along cycles of length 2s jump from nearly 0 in 2006 to ≈0.75 in 2010. We infer that diversification in equities assets is now difficult to achieve even at the 2s horizon. Moreover, the various industry sectors in the S&P 500 are now highly connected across all investment horizons. One might conclude that systemic risks in the market are now more serious than ever.

More generally, we observe a steady leftward shift of the curves in Figure 3-5 toward shorter cycle lengths. The peaks of the correlation spectra shift from cycle lengths of ≈10m in 2002 to ≈2m in 2006 to ≈30s in 2010. This phenomenon holds somewhat surprising implications. It suggests that in 2002, the shared underlying factors across all industry sectors were most active at the 10m horizon. Only eight years later in 2010, however, these shared factors were most significant along horizons of only 30s. It must be that the rise of high-frequency trading has either (1) generated new short-horizon financial dynamics that have supplanted the former ones, (2) shrunk the timescale along which many pre-existing financial and economic processes operate, or (3) a combination of the above.

Some distinctions beween sectors are worth discussing. Throughout the years we see that CNSMR exhibits the highest 1d-cycle correlation with TECH. This suggests that TECH stocks share more long-term factor exposures with CNSMR stocks than with other sectors. One explanation is that CNSMR is generally more correlated with the entire market, because the CNSMR sector includes retail and wholesale businesses. The performance of such businesses reflect the population's spending and

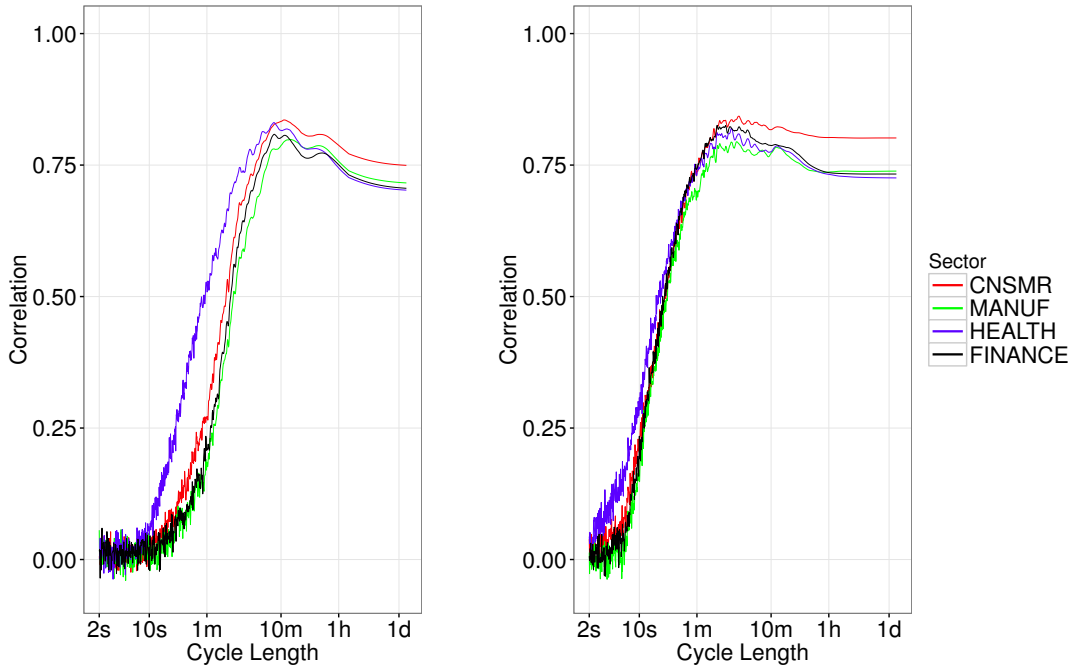

(a) 2002

(b) 2006

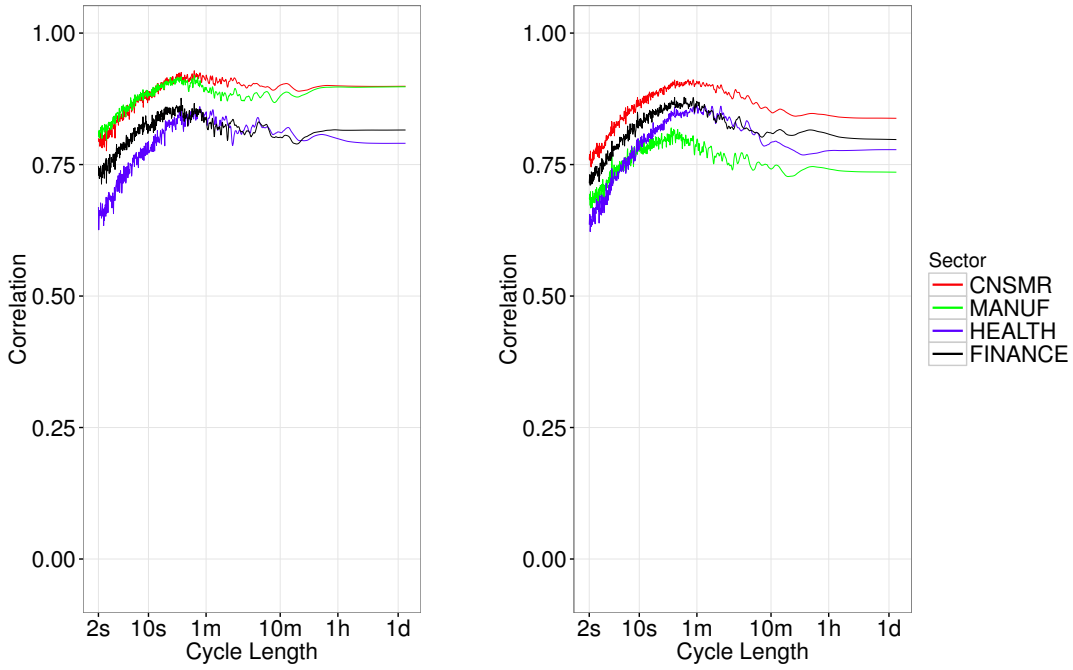

(c) 2010

(d) 2014

Figure 3-5: Smoothed correlation spectra between annual per-second returns of equal-weighted sector portfolios (containing subsets of S&P 500 constituents). The correlation spectra between the Technology portfolio and the Consumer, Manufacturing, Health, and Finance portfolios are graphed for the years (a) 2002, (b) 2006, (c) 2010, and (d) 2014.

disposable income, two factors that drive not only demand in other business but also general buying/selling pressure among retail investors.

Interestingly, Figure 3-5 shows that the distinctions between different sectors have grown more noticeable in the recent years. First, in 2010 and 2014 we observe more vertical separation between the curves, i.e. some sectors are more connected to TECH than others. Secondly, we also observe more horizontal separation, i.e. differentiation between the peak cycle lengths. For example, we see in 2014 that MANUF reaches its maximum correlation at shorter cycles than CNSMR and HEALTH. This suggests that TECH-MANUF share factor exposures along shorter horizons, while TECH-CNSMR and TECH-HEALTH share factor exposures along slightly longer horizons. It is possible that the increase in sector differentiation has been partially driven by the growth of exchange-traded funds (ETFs). ETFs allow investors to easily trade large baskets of stocks at once, and some of the most popular ETFs target specific sectors. Given the rise in ETF liquidity, it is now easier than ever for investors to execute sector-driven strategies. A growth in sector-driven trading would naturally contribute to sector differentiation.

Overall, however, we find that all of our sector portfolios behave relatively similarly. In each of the four years in Figure 3-5, the four spectrum curves exhibit similar shapes and exhibit peaks at comparable cycle lengths. This suggests that S&P 500 stocks across different sectors generally exhibit many shared trading characteristics. Finally, we briefly mention that HEALTH exhibits unusually high short-cycle correlations with TECH in 2002 and 2006, for which we have no explanation.

Chapter 4

Analysis of Contrarian Trading Strategies

In this chapter we apply our spectral framework to study the behavior of trading strategies. We focus solely on contrarian strategies (see Section 1.3) for two reasons. First, they are conceptually simple and already well-studied in the time domain. Second, the cyclical nature of buying losers and selling winners leads to intuitive properties in the frequency domain. Contrarian strategies are an ideal candidate for an intuitive illustration of our spectral analysis tools.

For each day across the years 1995-2014, we simulate contrarian trading strategies over the universe of the S&P Composite 1500 components. We consider the strategies that determine underperformers and overperformers over the past 1s, 10s, 1m, 10m, and 1hr.

In our simulation, all transactions occur at midpoint prices, and profits are marked to midpoints as well. Our historical strategy returns are thus inflated, because we ignore costs like crossing the bid-ask spread, price impact, and fees. For our purposes, however, we prefer to ignore microstructure effects, because it allows us to more cleanly interpret results in terms of overarching changes in price behaviors.

In Section 4.1, we first summarize the performance of the five contrarian strategies over the past two decades. Then, in Section 4.2 we decompose strategy profits into different frequencies, identifying a distinctive pattern of frequency exposures. Mo-

tivated by the results in Section 4.2, we propose a method of managing frequency exposures in Section 4.3.

4.1 Historical Returns

Figure 4-1 summarizes the annual performance of the five (1s, 10s, 1m, 10m, 1hr) contrarian strategies from 1995 to 2014. We graph the average unleveraged per-second returns across each year, as defined in Section 1.3.

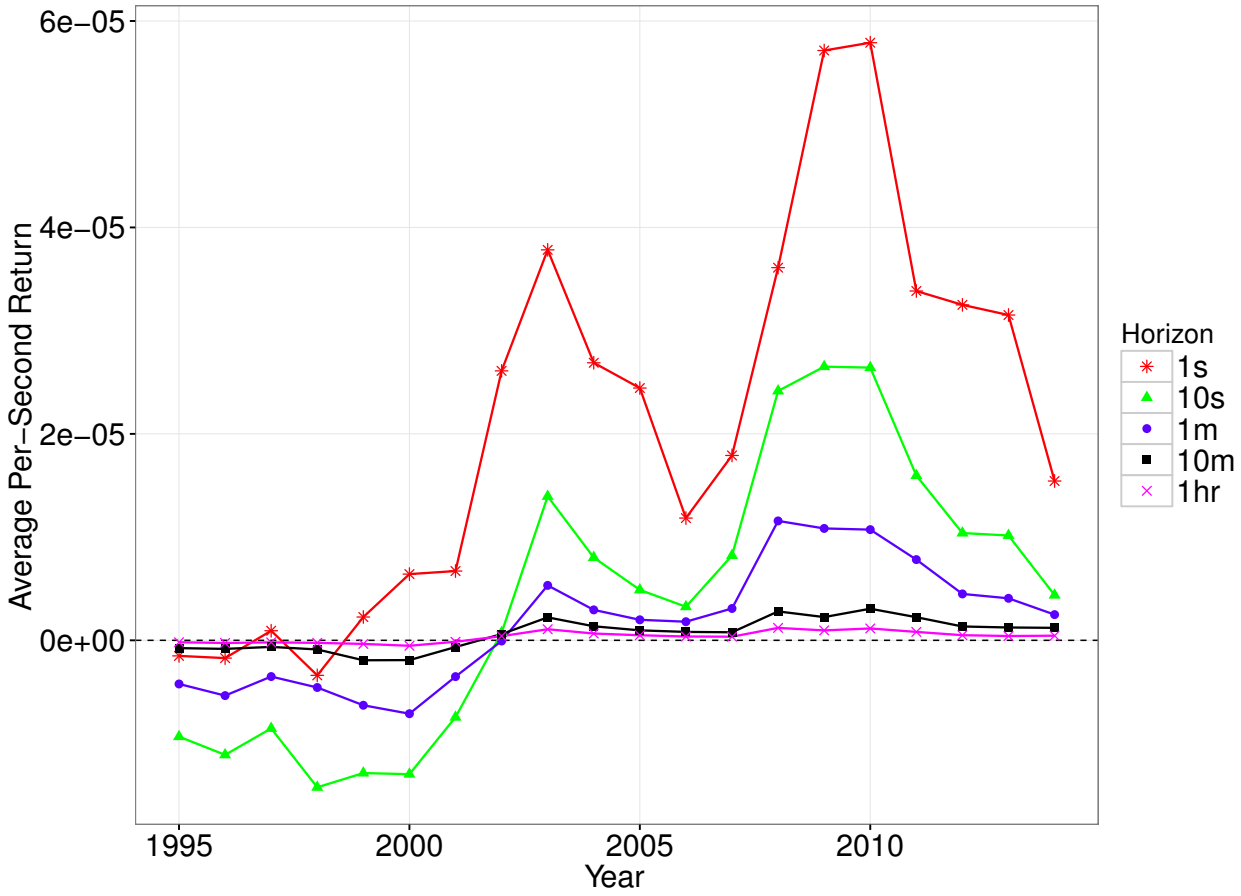

Figure 4-1: Annual averages of unleveraged per-second contrarian strategy returns, simulated over the universe of S&P 1500 constitutents, across the years 1995-2014. The T-horizon contrarian strategy determines overperformers and underperformers over the most recent length-T time interval.

The most striking pattern in Figure 4-1 is that the short-horizon strategies generate much higher returns. This is consistent with the high Sharpe ratios that are typi-

cally associated with high-frequency trading [5]. Upon seeing these results, one might wonder why many funds choose to operate on longer horizons instead of shorter. The answer is that although short-horizon strategies generate higher returns, they typically deploy only a small amount of capital. Generally speaking, large funds would be unable to fully invest their capital into high-frequency strategies.

We also observe a growth and decline in the 1s contrarian returns from 2006 to 2014, with a peak in 2009-10. This is encouragingly consistent with documented profits in the HFT industry, which are reported to have peaked in 2009 and fallen dramatically in subsequent years [52]. The extent to which our contrarian strategy returns align with documented industry performance suggests that our contrarian strategies successfully capture many elements of HFT behavior. Indeed, like high-frequency market makers, contrarian strategies are compensated for providing liquidity. The underperformance or overperformance of a stock is driven by an imbalance between buying and selling pressures. By buying underperformers and selling overperformers, contrarian strategies help stabilize these imbalances. This behavior is a form of liquidity provision, because it involves buying when the market wants to sell, and vice versa.

4.2 Frequency Decomposition of Profits

We now perform a frequency decomposition of profits with the tools described in Section 2.2.2. These tools help us understand the frequency exposure of a strategy, the cycles along which the strategy tends to gain profits or incur losses. Contrarian strategies naturally exhibit cyclical exposures, because of the dynamics of buying underperformers and selling overperformers. A frequency decomposition of contrarian profits leads to direct interpretations in terms of momentum and reversion.

In Figure 4-2, we present the frequency decomposition of the profits of the 1s, 10s, 1m, and 10m contrarian trading strategies. For each strategy, we consider the years 1995, 2000, 2005, and 2010. The most striking feature of the graphs is the oscillatory nature of the curves. For the T-horizon contrarian strategy, we see the highest profits

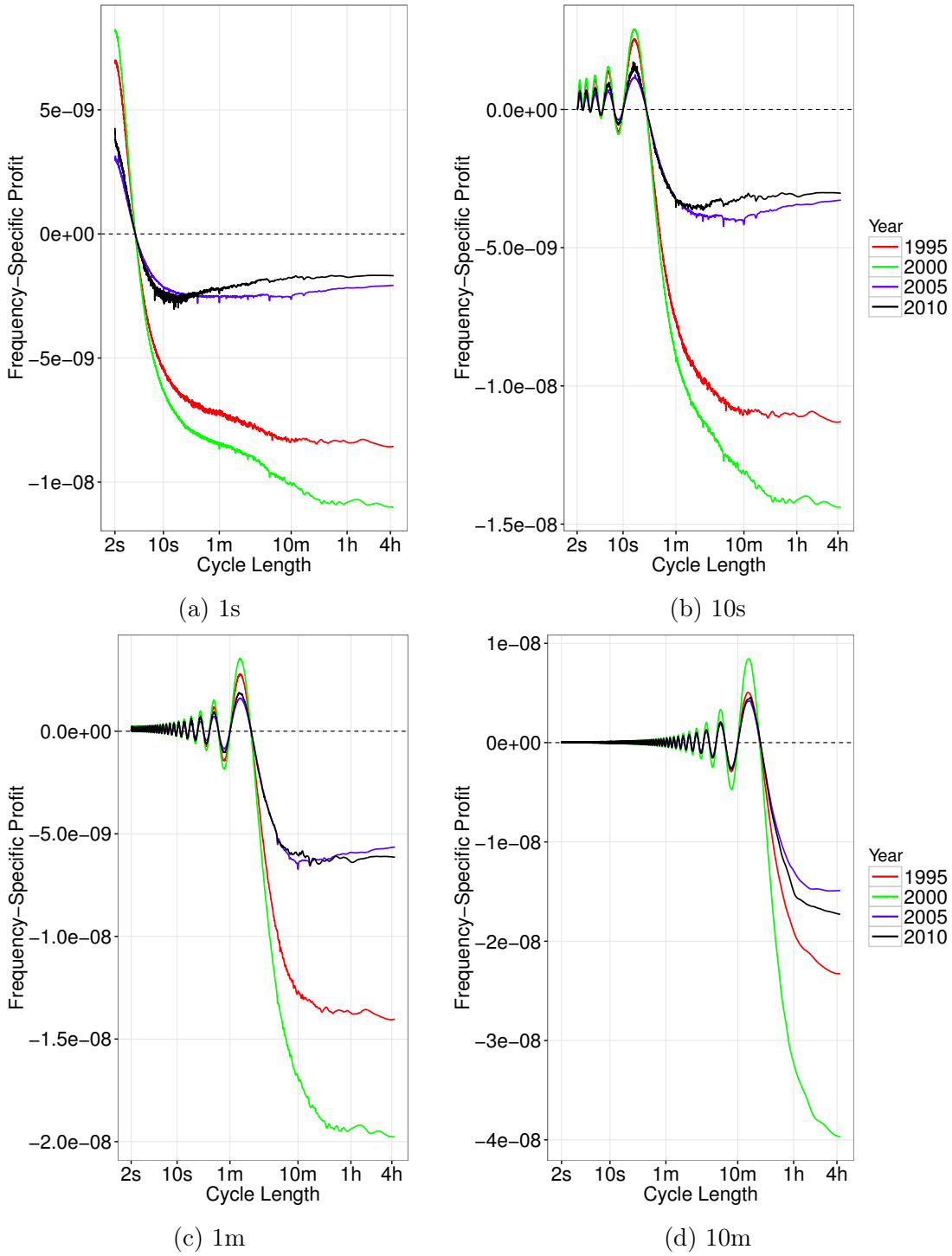

Figure 4-2: Unsmoothed frequency decomposition of contrarian strategy profits, simulated over the universe of S&P 1500 constituents, across the years 1995-2010. The profits of contrarian strategies at horizon lengths (a) 1s, (b) 10s, (c) 1m, and (d) 10m are graphed. The T-horizon contrarian strategy determines overperformers and underperformers over the most recent length-T time interval.

(the peak of the curves) along cycles of length $2T$. In addition, we see successively smaller peaks at harmonic frequencies corresponding to cycle lengths of $2T/3$, $2T/5$, $2T/7$, $2T/9$, etc.

This oscillatory structure in the frequency decomposition is no accident. The T-horizon contrarian strategy bets on mean reversion along a specific time scale. It bets on a negative correlation between the future return over the next timestep and the cumulative return over the past T timesteps. When we decompose the individual stock returns into a sum of sinusoidal cycles, the component of the returns that moves along cycles of length $2T$ naturally exhibits the most mean reversion against the past T timesteps. Similarly, the strategy also tends to be successful, to a lesser extent, when the returns move along the harmonic cycles of length $2T/(2k+1)$.

We also see in Figure 4-2 that all of the contrarian strategies incur heavy losses at long cycles. When returns move along sinusoidal cycles of length $\gg 2T$, the future return over the next timestep exhibits positive correlation with the cumulative return over the past T timesteps. As a result, the components of the returns associated with extremely long cycles always exhibit momentum with respect to the timescale of the strategy. Because the contarian strategy bets on mean reversion, it always suffers losses at those cycles. Also due to momentum effects, the contrarian strategy performs poorly at specific shorter cycle lengths as well.

Building on the intuition developed in the previous two paragraphs, we can interpret the performance of the T-horizon contrarian strategy as a trade-off between reversion and momentum. In Figure 4-1, we see that many of the contrarian strategies do not generate positive returns until 2002. The frequency decompositions in Figure 4-2 provide an explanation.

Across all horizons in Figure 4-2, the strategies actually produce more profits (i.e. more mean reversion) at the shorter cycles in 1995 and 2000 than in 2005 and 2010. However, in 1995 and 2000 the strategies suffer large losses from the strong cyclical activity at the longer cycles (i.e. strong momentum), producing net losses. On the other hand, in 2005 and 2010, the activity at longer cycles is not strong enough to outweigh the short-cycle gains, producing net profits. This leads us to conclude that

the improvement in contrarian strategy performance from pre-2002 to post-2002 is due to a reduction in long-cycle activity, rather than an increase in short-cycle activity.

Figure 4-2a also sheds light on the driving factors behind the growth of HFT profits from 2005 to 2010. The frequency decomposition of the 1s contrarian profits shows that from 2005 to 2010, the improvement in returns was driven by both a growth in short-cycle profits and a reduction in long-cycle losses.

4.3 Management of Harmonic Frequency Exposures

One implication of the frequency decompositions in Figure 4-2 is that the T-horizon contrarian strategy is exposed to short harmonic cycles. This unintended exposure to higher frequencies might be undesirable for investors whose expertise lies in identifying low-frequency trends. In this section, we illustrate how these high-frequency exposures can be removed from our contrarian strategy by incorporating a filter. The harmonic frequency exposures of a general trading strategy can be managed in the same manner.

In spectral estimation, a filter known as the Hamming window is often used to reduce spectral leakage, a problem that is analagous to the leakage of strategy exposure to harmonic frequencies. Motivated by these applications, we attempt to consolidate the frequency exposure of the contrarian strategy by filtering the cumulative returns from which we determine overperformers and underperformers.

Recall Equations 1.1 and 1.2, reproduced below, from the definition of our contrarian strategy in Section 1.3. The strategy is characterized by the following weights of a portfolio containing the universe of assets.

$$w_i[t] = R_m[t-T:t-1] - R_i[t-T:t-1]$$

$$R_m[t-T:t-1] = \frac{1}{N}\sum_{i=1}^{N} R_i[t-T:t-1]$$

$R_i[t-T:t-1]$ is defined as the cumulative return of the i-th asset over the timesteps

$t-T$, $t-T+1$, ..., $t-1$, as described in Equation 4.1.

$$R_i[t-T:t-1] = -1 + \prod_{n=0}^{T-1}(1+R_i[t-T+n]) \approx \sum_{n=0}^{T-1} R_i[t-T+n] \tag{4.1}$$

We formulate a *filtered* contrarian strategy by replacing $R_i[t-T:t-1]$ with $R'_i[t-T:t-1]$, the dot product of the returns series and a filter $w[n]$, shown in Equation 4.2.

$$R'_i[t-T:t-1] = \sum_{n=0}^{T-1} R_i[t-T+n]w[n]. \tag{4.2}$$

Motivated by spectral estimation applications, we choose the filter $w[n]$ to be the Hamming window in Equation 4.3.

$$w[n] = 0.54 - 0.46\cos\left(\frac{2\pi n}{T-1}\right). \tag{4.3}$$

This characterizes our new *filtered* T-horizon contrarian strategy:

$$w_i[t] = R'_m[t-T:t-1] - R'_i[t-T:t-1] \tag{4.4}$$

$$R'_m[t-T:t-1] = \frac{1}{N}\sum_{i=1}^{N} R'_i[t-T:t-1]. \tag{4.5}$$

Next, we empirically illustrate the degree to which our filtering technique reduces harmonic frequency exposures. Figure 4-3 compares the frequency decomposition of the profits of the original 1m contrarian strategy against the filtered 1m contrarian strategy over the year 2014. We see that our filtering technique virtually eliminates the exposure to harmonic frequencies. The filtered strategies at other horizons and in other years exhibit nearly identical results. The filtered T-horizon contrarian strategy consolidates the mean reversion profits to cycle lengths of approximately $2T$ and maintains the momentum-induced losses at longer cycles.

The application of a filter to reduce harmonic frequency exposures extends beyond contrarian trading strategies. This technique can be utilized in any general trading strategy that adjusts weights based on a cumulative return over the past T timesteps.

By replacing the cumulative return with a filtered sum, a low-frequency investor can eliminate undesired exposures to higher frequencies.

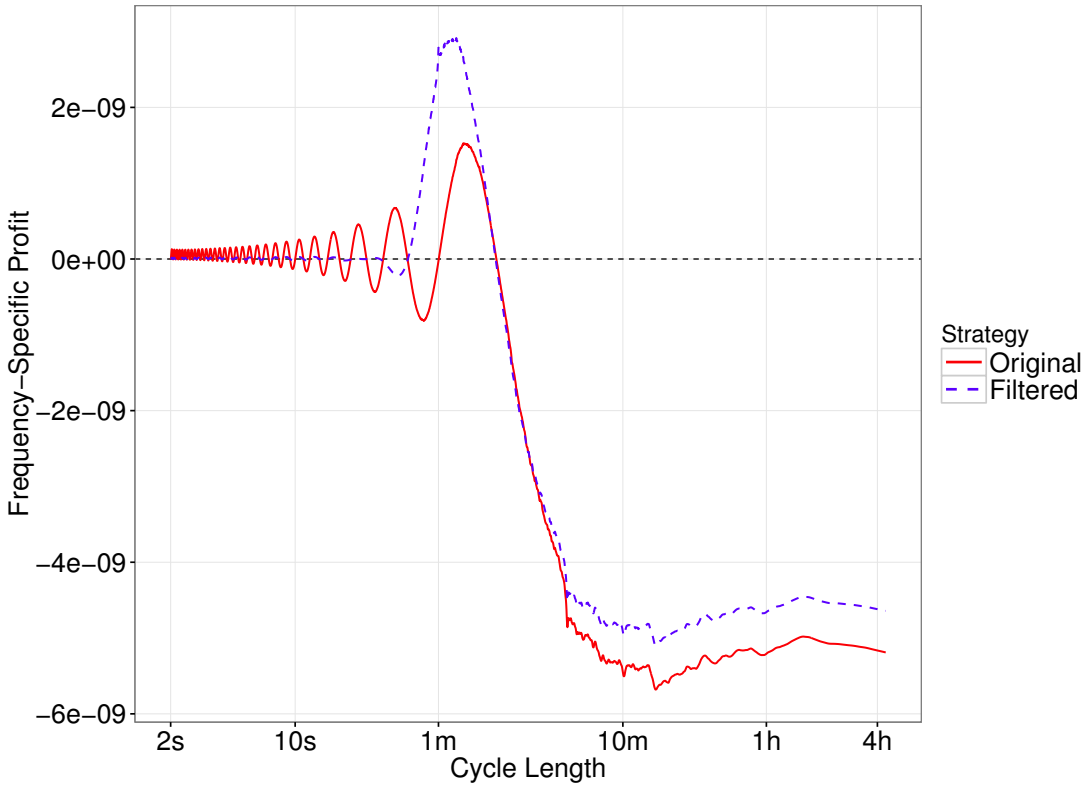

Figure 4-3: Unsmoothed frequency decomposition of original and filtered 1m contrarian strategy profits, simulated over the universe of S&P 1500 constituents, in the year 2014.

Chapter 5

Analysis of Market Stress Events

In this chapter, we examine a few major market stress events of the past decade, using techniques established earlier. We compare market behaviors before and after these events, in terms of the correlation spectrum and contrarian strategy profits. Such a comparison allows us to theorize about how market participants respond to and are affected by these events.

A before-versus-after comparison is most appropriate for studying sudden, discrete shocks. It is more difficult to perform this analysis for long-term events because of confounding variables. For example, consider a sustained event such as the 2007-2008 financial crisis. As impactful as the event was, the financial markets also underwent other fundamental changes over the crisis years, such as the surge of high-frequency trading, that are at least somewhat orthogonal to the crisis. Consequently, it would be challenging to attribute differences between pre- and post-crisis market behaviors to the crisis itself. Furthermore, even if a cause-effect relationship could be established, it would not necessarily be meaningful. Sustained events such as the 2007-2008 financial crisis tend to induce extensive and complex effects, muddling the attribution of behavioral changes to a specific aspect of the event.

Because of these complications, we choose to focus our analysis to brief, sudden shocks that transpired over the course of a single day or a few days. We study the following four events.

1. **Chinese Correction: February 27, 2007**, a day on which a 9% plunge in the Shanghai SSE Composite Index led a global dive. The initial Chinese crash was driven by speculation about government policy.

2. **Quant Meltdown: August 6-10, 2007**, a week over which many supposedly beta-neutral quantitative funds experienced massive losses. Other segments of the financial industry were virtually unaffected.

3. **Flash Crash: May 6, 2010**, a day on which the DJIA fell 600 points within 5 minutes, only to regain most of the drop after another 20 minutes. Shares of some S&P 500 stocks traded at prices as low as $0.01 and others as high as $100,000.

4. **Black Monday 2011: August 8, 2011**, a day on which the NASDAQ Composite Index lost nearly 7% after S&P downgraded the rating of US soverign debt from AAA to AA+.

In Section 5.1, we first provide a brief summary of the four events. Afterwards, in Section 5.2 we perform our analysis and discuss results.

5.1 Brief Overview of Events

5.1.1 Chinese Correction: February 27, 2007

Driven by economic growth, Chinese markets exhibited stellar performance through the latter half of 2006. However, the turn of the year brought a wave of volatility, marked by a slump at the end of January and through the beginning of February.

Chinese markets appeared to have weathered the storm, after the Shanghai SSE Composite Index regained losses and later reached an all-time high on February 26. However, the SSE dropped nearly 9% on the very next day, February 27, on rumors of impending financial policies from the Chinese government. The rumored policies ranged from a crackdown on trading with borrowed money to increases in interest rates to tax reforms [2].

The Chinese crash on February 27, known as the Chinese Correction, triggered a global panic. It is possible that US markets were already uneasy, because on the previous day Greenspan had expressed fears of an imminent US recession [1]. Regardless, the DJIA followed the Chinese Correction with a 3.3% fall, at the time its biggest one-day loss since September 11. Europe opened at large losses as well [57]. Overall, the crash induced anxiety among investors around the world. Some feared that the Chinese Correction signaled a regime shift in Asian markets, while others insisted that economic fundamentals remained strong and attributed the crash to speculation [2].

It appears that the latter opinion was more correct, because the SSE Index recovered steadily after the crash, setting a new all-time high only three weeks later. The Chinese Correction is an ideal candidate for a before-versus-after comparison, because it appears to have been an isolated event. Through an analysis of this event we can study the impact of a foreign shock on US stocks.

5.1.2 Quant Meltdown: August 6-10, 2007

The most prominent financial events in 2007 were those involved in the buildup to the 2007-2008 financial crisis. In the midst of these high-profile macroeconomic developments, however, a rather bizarre event occured during the week of August 6-10, known as the Quant Meltdown.

During that week, some of the world's most reputed quantitative, model-driven funds experienced massive losses. Two of Goldman Sach's funds, its Global Equity Opportunities fund and Global Alpha fund, respectively lost approximately 30% and 15% over the week [3]. On August 10, AQR's flagship fund was down 13% on the month [50], and even the Renaissance Technologies Medallion fund, which averaged an astounding 71.8% annual before-fees return from 1994 to 2014 [54], had lost 8.7% on the month [60].

Meanwhile, other segments of the financial industry were not noticeably affected. Many quantitative hedge funds claim to implement superior management of market factor exposures, and the sweeping wave of losses that specifically disturbed quanti-

tative funds raised questions about the true nature of their risks.

Less than two months later in late September, Khandani & Lo [38] proposed a now widely-accepted explanation for the events. They hypothesized that the meltdown was driven by a liquidation spiral, initially triggered by a sudden and possibly forced unwinding of at least one quantitative portfolio. With many funds deploying similar quantitative long/short equity strategies, it is possible that a crowded quant niche was heavily interconnected by shared exposures. A sudden initial liquidation would have exerted strong selling pressures, pushing firms with shared exposures to their risk limits. As a result, those firms could have been forced to de-leverage or even liquidate, furthering the cycle.

One telltale sign of a liquidity shock is a swift recovery after the spiral runs its course and the market imbalances subside. Indeed, many of the unprecedented losses during the Quant Meltdown were regained just as suddenly as they were lost. Within two weeks, the AQR fund had regained half of its losses, and the Renaissance Medallion fund was rumored to have recovered completely [50]. The Quant Meltdown appears to have been an idiosyncratic, isolated blip on the radar.

Despite its minimal macroeconomic relevance, the Quant Meltdown undoubtedly had a dramatic impact on players within the quantitative space, forcing the industry to reassess their characterizations of risk. Any changes in market behavior revealed in a before-versus-after analysis could be potentially associated with the adapation of quantitative hedge funds.

5.1.3 Flash Crash: May 6, 2010

On the morning of May 6, 2010, the US markets opened at a loss over anxiety about the Greek Debt Crisis and continued to trend downwards. Then suddenly in the afternoon, the DJIA tumbled 600 points in the 5-minute span from 2:42pm to 2:47pm [58], erasing $1 trillion of market value [37]. This free-fall at superhuman speeds is known as the Flash Crash. Many S&P 500 stocks briefly traded at absurd prices; some like Accenture traded at $0.01 [41], while others like Apple and Hewlett-Packard traded at over $100,000 [45]. Many of these trades were later cancelled.

Just as shocking as the fall itself, the markets rebounded with unprecedented speed, with the DJIA regaining nearly all of the 600-point dive within 20 minutes by 3:07pm [37]. By the close less than an hour later, the market returned to an “almost a normal, quiet day at the end", according to a former COO at EWT Trading [37].

The Flash Crash is considered one of the most mysterious market events to have ever occured. Over half a decade later, experts are still far from consensus on an explanation for the events. In 2015, the US Department of Justice arrested Navinder Singh Sarao, a small-time trader working from a house in suburban London, for his role in instigating the crash. Sarao attempted to manipulate the S&P 500 E-mini futures market by flooding it with $200 million’s worth of sell orders (about a quarter of all sell orders in the market) that he planned to cancel, creating the false impression of an order imbalance that the Securities and Exchange Commision (SEC) and the Commodities Futures Trading Commission (CTFC) claim were a driving element of the crash [13]. Some have expressed doubts about the degree to which a single independent trader could be responsible.

To some, the Flash Crash exemplifies the deep dangers that automated and high-frequency trading pose to market stability. A CTFC report contends that although high-frequency traders did not technically cause the crash, they exacerbated its effects [39]. Given its severity and abruptness, the Flash Crash indubitably elicited reactions from automated and manual traders alike. A before-versus-after analysis might illustrate the impact of the general unease with market structure that followed the event.

5.1.4 Black Monday 2011: August 8, 2011

In 2011, the US Congress engaged in fierce debate over the raising of the federal debt ceiling, which requires approval in both the House of Representatives and the Senate. Members across the aisle, many Republicans and some Democrats, refused to approve any increase in the debt ceiling without a reduction of the federal deficit. However, the two parties sharply differed in deficit reduction plans. The Republicans, partially influenced by the Tea Party, rejected any tax increases and demanded large cuts in

spending. On the other hand, the Democrats insisted on tax increases and smaller spending cuts [35].

The debt ceiling itself does not commit the federal government to additional spending – it only authorizes the payment of debts that the federal government has already commited to. The US Treasury estimated that borrowing authority of the federal government would have been exhausted on August 2 [49]. If no agreement on a debt ceiling raise were reached by this date, the federal government would have possibly been forced to default on its debt and spark a financial crisis.

Although an agreement that involved $2.4 trillion in deficit cuts was eventually reached on July 31, the inability of Congress to negotiate a deal before the eleventh hour disturbed many. Financial agencies began to question the conventional designation of US federal debt as risk-free. Before the agreement was made, on July 28 the ratings agency Standard & Poor's (S&P) had warned that any deficit cuts less than $4 trillion would jeopardize its AAA risk-free rating of the US government [20]. On August 1, Moody's Investors Service cautioned that the "outlook for the US grade is now negative" [19]. Finally on the night of Friday, August 5, S&P downgraded the AAA rating to AA+ [21].

The markets responded emphatically the following business day on August 8, known as Black Monday 2011. The S&P 500 Index plunged 6.6%, leading retreats in markets around the world. The downgrade of US debt spurred debate over the AAA ratings of British and French debt as well [12]. Combined with general developments in the European sovereign debt crisis, these events delivered market volatility throughout the rest of August and through much of the rest of the year. A before-versus-after analysis of Black Monday 2011 might capture general elements of market behaviors after macroeconomic shocks.

5.2 Event Analysis

Now we perform a before-versus-after analysis of the four events. Our analysis consists of two components. First, in Section 5.2.1 we study changes in the correlation

spectrum between pairs of S&P 500 stocks. Afterwards, in Section 5.2.2 we study the daily performance of contrarian strategies around the events.

5.2.1 Correlation Spectrum

We study the three weeks before and the three weeks after each event. For each day in those six weeks, we compute the average correlation spectrum between all pairs of S&P 500 stocks. Then, we aggregate the daily results to produce weekly averages, shown in Figure 5-1.

In Figure 5-1, the dashed curves represent the three weeks before the events, and the solid curves represent the three weeks after. The weeks after the Chinese Correction, the Flash Crash, and Black Monday 2011 exhibit sustained spikes in correlations across all cycle lengths, with larger increases along longer cycles. On the other hand, the weeks after Quant Meltdown do not. A major difference between the Quant Meltdown and the other events is that the Quant Meltdown only shocked a very specific niche within the industry, while the other events generated deep anxiety across global markets.

We hypothesize that stocks in the S&P 500 only become highly correlated in the presence of strong universal risks. During these stresses, long-term players must adapt to the events and predict macroeconomic trends. Short-term players must adapt to increased volatility and anticipate potential regime shifts. In the case of the Chinese Correction and Black Monday 2011, the macroeconomic risks of a Chinese crash and a US credit downgrade concerned nearly all market participants. Similarly, the structural risks highlighted by the Flash Crash drew urgent attention across virtually all financial niches.

In the presence of universal risks that impact all market players and all assets, factors that are company-specific or even industry-specific tend to become relatively less significant. A large portion of stock variance becomes driven by the same risk factors, producing higher correlations across all cycle lengths. On the other hand, when no urgent risk factors are universally relevant, we expect company-specific and industry-specific factors to account for a larger fraction of stock variance. Risk be-

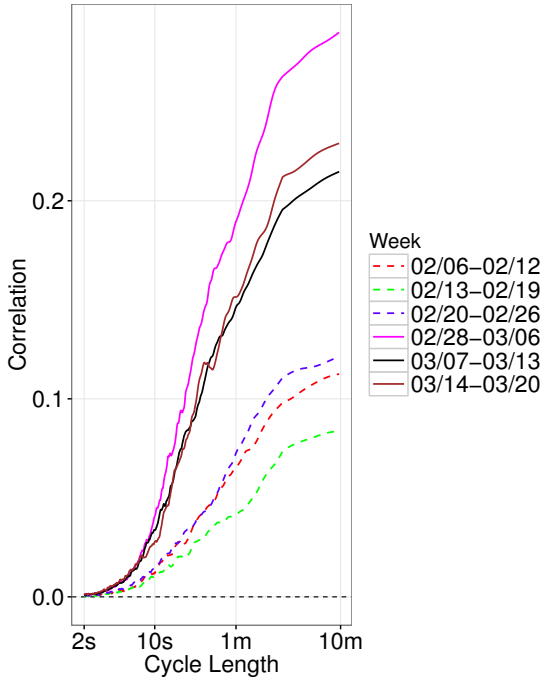

(a) Chinese Correction

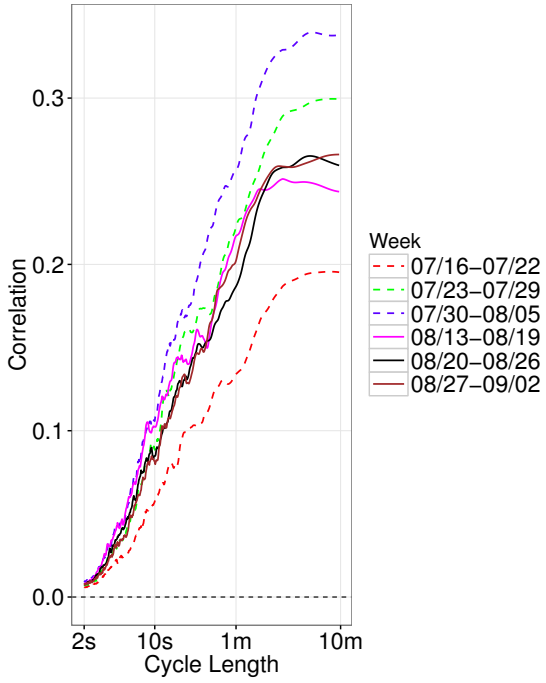

(b) Quant Meltdown

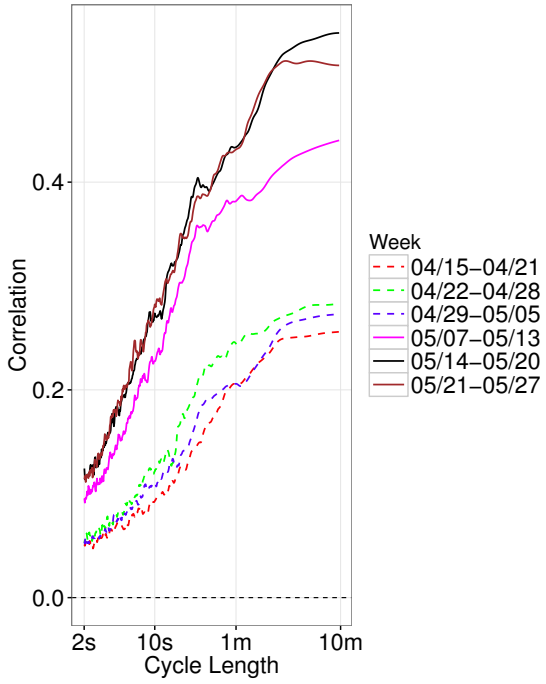

(c) Flash Crash

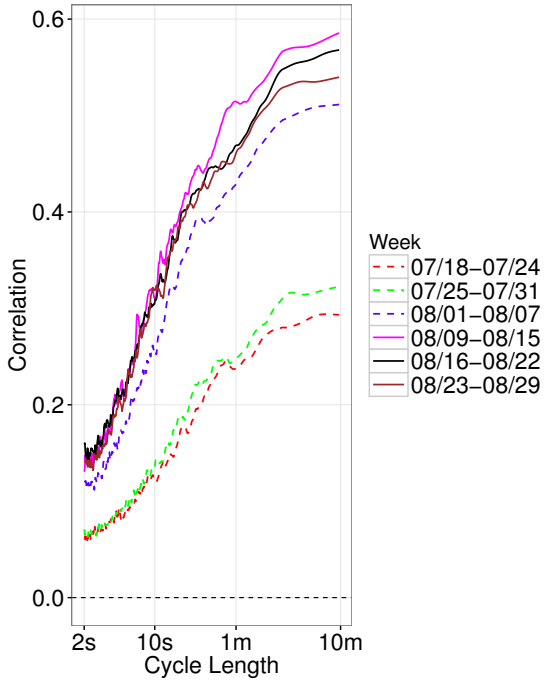

(d) Black Monday 2011

Figure 5-1: Smoothed correlation spectra between weekly per-second stock returns, averaged across all pairs of S&P 500 constituents, during the three weeks before and the three weeks after (a) the Chinese Correction, (b) the Quant Meltdown, (c) the Flash Crash, and (d) Black Monday 2011.

comes dissipated across a wider range of factors, producing lower average correlations between stocks.

Likely because Quant Meltdown did not demonstrate any universal risks to the wider industry, we see no increase in correlations after the event. However, other characteristics of Figure 5-1b are worth noting. It appears that the correlation spectrum becomes more stable in the three weeks after the Quant Meltdown, exhibiting less week-to-week variation. While it is very possible that this six-week trend is pure coincidence, it is also possible that the quantitative space adapted in a way that produced a more stable correlation spectrum.

Finally, we observe that in Figure 5-1d, the correlation spectrum rises during the week *before* S&P's downgrade and the subsequent crash on August 8. A likely explanation is that by the week of August 1, the market had already recognized the prospect of a US credit downgrade as a universal risk. This is unsurprising, since speculation of a downgrade had grown for weeks, and Moody's issued explicit warnings of a downgrade on August 1 (see Section 5.1.4).

5.2.2 Contrarian Strategy Returns

The second component of our event analysis is a review of contrarian strategy returns. For each of the four events, we compute the daily average per-second contrarian returns over the two months around the event. The contrarian strategies, as defined in Section 1.3, are implemented over the universe of S&P Composite 1500 stocks. Results are presented in Figure 5-2. Figure 5-2c does not include the extreme returns on May 6, the day of the Flash Crash. Those returns are not meaningful, because most of the high-impact trades were later cancelled by exchanges.

Figure 5-2 shows increased contrarian returns during and after the Chinese Correction, the Flash Crash, and Black Monday 2011. This is consistent with the intuition that strategy returns should grow during periods of high volatility, because larger price movements present larger opportunities. We also see that the US credit downgrade prompted a more extended period of increased returns than the Chinese Correction and the Flash Crash. We provide an explanation in the next paragraph.

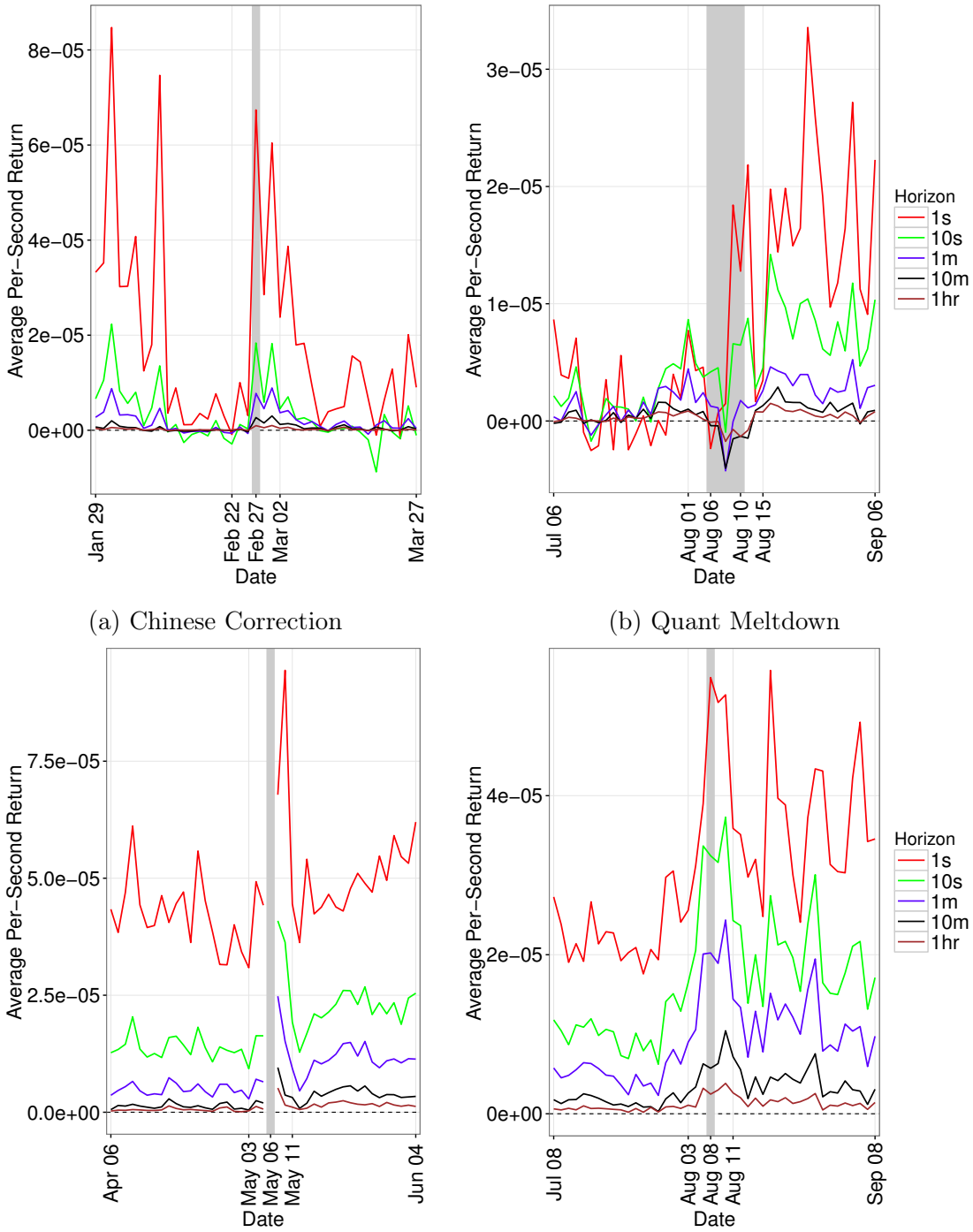

(a) Chinese Correction

(b) Quant Meltdown

(c) Flash Crash

(d) Black Monday 2011

Figure 5-2: Daily averages of unleveraged per-second contrarian strategy returns, simulated over the universe of S&P 1500 constitutents, during the days surrounding (a) the Chinese Correction, (b) the Quant Meltdown, (c) the Flash Crash, and (d) Black Monday 2011. The T-horizon contrarian strategy determines overperformers and underperformers over the most recent length-T time interval.

The time interval over which we see increased contrarian returns reflects the strength of the event's long-term effects. The US credit downgrade directly affected macreconomic fundamentals of the global economy, leading to more sustained effects. Although the Chinese Correction also sparked worries around the world, investors saw no obvious changes in the fundamentals of the Chinese economy. After the SSE Index recovered steadily over the following days, many attributed the crash entirely to speculative selling pressures. Finally, in Figure 5-2c we observe that the Flash Crash led to only a brief period of increased returns. Because the losses during the Flash Crash were regained within 20 minutes, most determined that the crash was purely a structural breakdown. After two days of stable trading to end the week, market participants likely concluded that the Flash Crash was an idiosyncratic event with minimal long-term implications.

We conclude our analysis with a discussion of the Quant Meltdown in Figure 5-2b. Already seen in Section 4.1, the contrarian strategies along longer horizons tend to produce much lower returns. As a result, it is likely that the quantitative funds operating at hourly or daily horizons rely on leveraging to magnify returns. Unfortunately, leveraging magnifies losses as well. During the week of August 6-10, the 10m and 1hr contrarian strategies could have produced devastating returns if leveraged. On August 8 we even see large losses from the 1m strategy, which typically produces high returns.

The performance of strategies depicted in Figure 5-2b bears striking resemblance to documented returns during the Quant Meltdown. Following the abysmal week, the strategies achieve strong returns throughout the rest of the month. We theorize that the Quant Meltdown triggered the exit of many funds, temporarily reducing competition within the quant space and increasing the returns of quantitative strategies.

Chapter 6

Conclusions

In this paper, we have demonstrated the application of frequency domain methods to financial analysis. We showed how Parseval's Theorem can be used to decompose quantities like covariance and trading strategy performance into frequency-specific components. Since each frequency component is associated with cycles of a particular length, the frequency decomposition naturally facilitates the interpretation of financial quantities in terms of horizon-specific behaviors.

At the very least, these spectral techniques enable a computationally efficient analysis of behaviors across a wide spectrum of horizons. Additionally, we argue that a spectral framework for horizon-specific analysis is much less susceptible to undesirable aliasing effects than conventional time-domain methods. Overall, a spectral framework might be better equipped to study processes that contain inherently cyclic components (e.g. business cycles, credit cycles, liquidity cycles, etc.).

Using these frequency domain methods, we performed an empirical analysis of high-frequency dynamics in per-second data over the years 1995-2014, and the methods produced interpretable results. We first studied the behavior of returns. We found that the frequency decomposition of individual stock variance and portfolio variance captures the shift into higher-frequency activity driven by the rise of electronic trading. In an analysis of Coca-Cola, PepsiCo, Exxon Mobil, and Southwest Airlines, we discovered that the shape of the correlation spectrum reflects the types of shared market exposures. In a study of market cap portfolios, we concluded that

large-cap, mid-cap, and small-cap stocks are driven in the long term by similar economic factors. In the short-term, we characterized behavioral differences in terms of liquidity factors. Finally, we studied the behaviors of different sector portfolios and attributed trends to the growth of ETFs.

We also studied the spectral behavior of contrarian trading strategies, simulated over the S&P Composite 1500. Since our simulated results aligned closely with the documented historical performance of the HFT industry, we inferred that the contrarian strategy captures many real dynamics of high-frequency traders. We developed an intuitive interpretation of the frequency decomposition of profits in terms of mean reversion and momentum, and this interpretation allowed us to attribute historical changes in contrarian profits to separate components. Additionally, we discovered that the adjustment of portfolio weights based on a cumulative past return exhibits exposure to harmonic frequencies. To eliminate these unintended higher-frequency exposures, we introduced a filtering technique and demonstrated its application to the contrarian strategy.

We concluded our empirical studies with an analysis of recent market stress events. We identified four sudden market shocks and compared market behaviors during the weeks before and the weeks after these events. After examining the average correlation spectrum betwen pairs of S&P 500 stocks, we theorized about conditions under which assets become highly connected. An analysis of contrarian profits revealed differences between the events in terms the duration of their impact.

Given the interpretable nature of frequency domain methods and the intuitive empirical results that they have produced, we conclude that spectral analysis demonstrates high potential for financial applications. In this paper, we have mostly focused on the analysis of historical behaviors, but a spectral perspective might be valuable in other areas as well. The notions of horizon-specific variance and correlation hold implications for portfolio optimization and risk management. For example, these horizon-specific quantities could serve as direct inputs in the framework of mean-variance optimization. In addition, one might argue that the frequency exposure of a portfolio is a fundamental dimension of risk that should be diversified and managed.

Finally, we note that a Fourier framework exhibits fundamental weaknesses. For example, the trade-off between frequency resolution and time resolution can be difficult to manage. Furthermore, a Fourier framework is most appropriate for capturing cycles that are sinusoidal. However, many financial cycles are not sinusoidal – for example, portfolio managers tend to adjust weights at discrete time invervals. A spectral framework based on wavelet analysis might be ultimately superior.

Appendix A

Data Issues

The two main flaws in our data are (1) errors in the TAQ database and (2) incomplete historical index constituents.

Handling TAQ Errors via Outlier Removal

Given the enormous amount of tick data in the TAQ database, it is unsurprising that it contains some errors. Some errors are isolated ticks, while others recur frequently throughout minute-long or even day-long intervals. In an attempt to manage these errors, we remove outliers.

For any given stock on any full trading day, we compute the midpoint price and the spread at each of the 23,400 seconds in the day. We determine that a particular second of the day is an outlier if it satisfies any of the conditions below. These rules were developed through a manual examination of incorrect data and correct data during extreme market events.

1. The absolute return over the past second is greater than 8%.

2. The absolute return over the past second is greater than 10 times the 20th largest absolute return over any second in the day.

3. The spread is larger than 100 times the median spread across all seconds in the day.

If a stock exhibits more than 100 outliers within a single day, then we remove the entire day's worth of returns for that stock.

Incomplete Historical Index Constituents

Although the S&P Compustat database contains historical index constituents, it only provides the present-day ticker symbols of those stocks. On the other hand, historical data in the TAQ database can only be retrieved with the historical ticker symbol. The present-day and historical ticker symbols can differ because of ticker changes over time. Some ticker changes are specifically requested, while others are due to mergers or split-ups. The further we look into the past, the more likely it is that a company's ticker has changed since then. Figure A-1 shows the number S&P 1500 and S&P 500 constituents that we are able to retrieve from TAQ across 1995-2014.

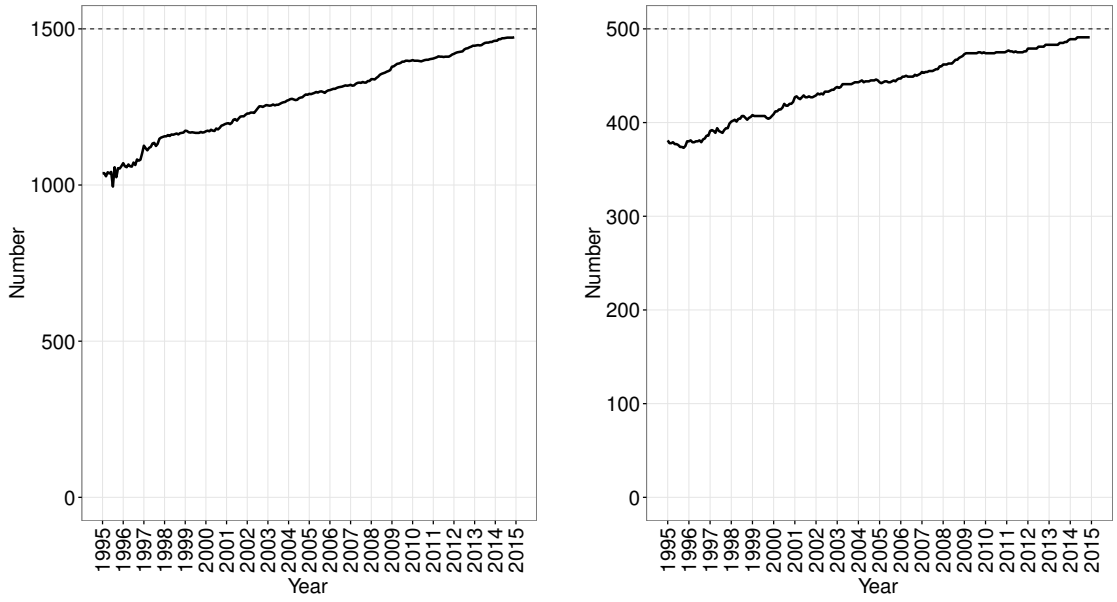

(a) S&P 1500 (b) S&P 500

Figure A-1: Number of retrieved constituents of (a) the S&P Composite 1500 Index and (b) the S&P 500 Index across the years 1995-2014.

Appendix B

Allocation of SIC Codes to Sectors

Cnsmr	Manuf	Tech	Health	Finance	Other
100-999	1200-1399	3570-3579	2830-2839	6000-6999	All Other Codes
2000-2399	2520-2589	3622-3622	3693-3693		
2500-2519	2600-2699	3660-3692	3840-3859		
2590-2599	2750-2769	3694-3699	8000-8099		
2700-2749	2800-2829	3810-3839			
2770-2799	2840-2899	4800-4899			
3100-3199	2900-2999	7370-7372			
3630-3659	3000-3099	7373-7373			
3710-3711	3200-3569	7374-7374			
3714-3714	3580-3621	7375-7375			
3716-3716	3623-3629	7376-7376			
3750-3751	3700-3709	7377-7377			
3792-3792	3712-3713	7378-7378			
3900-3939	3715-3715	7379-7379			
3940-3989	3717-3749	7391-7391			
3990-3999	3752-3791	8730-8734			
5000-5999	3793-3799				
7200-7299	3860-3899				
7600-7699	4900-4949				

Table B-1: Allocation of Standard Industrial Classification (SIC) codes to industry sectors.

References

[1] Greenspan fears recession - report. *CNN Money* (2007).

[2] Share sale knocks chinese market. *BBC News* (2007).

[3] Anderson, J. Goldman and investors to put $3 billion into fund. *New York Times* (2007).

[4] Ball, R., Kothari, S., and Shanken, J. Problems in measuring portfolio performance an application to contrarian investment strategies. *Journal of Financial Economics 38*, 1 (1995), 79–107.

[5] Baron, M., Brogaard, J., Hagstromer, B., and Kirilenko, A. A. Risk and return in high-frequency trading.

[6] Bartlett, M. S. Smoothing periodograms from time-series with continuous spectra. *Nature 161* (1948), 686–7.

[7] Baxter, M., and King, R. G. Measuring business cycles: Approximate band-pass filters for economic time series. *The Review of Economics and Statistics 81*, 4 (November 1999), 575–93.

[8] Bernard, V. L., and Thomas, J. K. Evidence that stock prices do not fully reflect the implications of current earnings for future earnings. *Journal of Accounting and Economics 13*, 4 (December 1990), 305–40.

[9] Beveridge, W. H. Weather and harvest cycles. *The Economic Journal 31*, 124 (December 1921), 429–452.

[10] Beveridge, W. H. Wheat prices and rainfall in Western Europe. *Journal of the Royal Statistical Society 85*, 3 (May 1922), 412–75.

[11] Bloomfield, P. *Fourier Analysis of Time Series: An Introduction*. John Wiley & Sons, 2004.

[12] Bremer, C., and Dmitracova, O. Analysis: France, Britain AAA-ratings under scrutiny. *Reuters* (2011).

[13] Brush, S., Schoenberg, T., and Ring, S. How a mystery trader with an algorithm may have caused the Flash Crash. *Bloomberg* (2015).

[14] Cao, C., Hansch, O., and Wang, X. The information content of an open limit-order book. *The Jounral of Futures Markets 29*, 1 (2009), 16–41.

[15] Chaudhuri, S. E., and Lo, A. W. Spectral analysis of stock-return volatility, correlation, and beta. *IEEE Signal Processing and Signal Processing Education Workshop (SP/SPE)* (2015), 232–6.

[16] Chaudhuri, S. E., and Lo, A. W. Spectral portfolio theory. Working Paper, April 2016.

[17] Conrad, J., and Kaul, G. Long-term market overreaction or biases in computed returns? *The Journal of Finance 48*, 1 (March 1993), 39–63.

[18] Croux, C., Forni, M., and Reichlin, L. A measure of comovement for economic variables: Theory and empirics. *The Review of Economics and Statistics 83*, 2 (May 2001), 232–41.

[19] Detrixhe, J. Moody's, Fitch affirm U.S. ratings while warning of downgrades. *Bloomberg* (2011).

[20] Detrixhe, J. U.S. $4 trillion deficit cut is 'good down payment,' S&P says. *Bloomberg* (2011).

[21] Detrixhe, J. U.S. loses AAA rating at S&P on concern debt cuts deficient. *Bloomberg* (2011).

[22] Engle, R. F. Band spectrum regression. *International Economic Review 15*, 1 (February 1974), 1–11.

[23] Fama, E. F., and French, K. R. Business conditions and expected returns on stocks and bonds. *Journal of Financial Economics 25* (1989), 23–49.

[24] Fama, E. F., and French, K. R. The cross-section of expected stock returns. *The Journal of Finance 47*, 2 (June 1992), 427–65.

[25] Fama, E. F., and French, K. R. Common risk factors in the returns on stocks and bonds. *Journal of Financial Economics 33* (1993), 3–56.

[26] Granger, C. W. J. The typical spectral shape of an economic variable. *Econometrica 34*, 1 (January 1966), 150–61.

[27] Granger, C. W. J., and Engle, R. Applications of spectral analysis in econometrics. *Handbook of Statistics 3* (1983), 93–109.

[28] Granger, C. W. J., and Hatanaka, M. *Spectral analysis of economic time series*. Princeton University Press, 1964.

[29] Granger, C. W. J., and Morgenstern, O. Spectral analysis of New York stock market prices. *Kyklos 16*, 1 (February 1963), 1–27.

[30] Grinblatt, M., Titman, S., and Wermers, R. Momentum investment strategies, portfolio performance, and herding: A study of mutual fund behavior. *The American Economic Review 85*, 5 (December 1995), 1088–1105.

[31] Hannan, E. J. Regression for time series with errors of measurement. *Biometrika 50*, 3/4 (December 1963), 293–302.

[32] Hasbrouck, J., and Sofianos, G. The trades of market makers: An empirical analysis of NYSE specialists. *The Journal of Finance 48*, 5 (December 1993), 1565–93.

[33] Hodrick, R. J., and Prescott, E. C. Postwar U.S. business cycles: An empirical investigation. *Journal of Money, Credit and Banking 29*, 1 (February 1997), 1–16.

[34] Huang, R. D., and Stoll, H. R. Market microstructure and stock return predictions. *Review of Financial Studies 7*, 1 (1994), 179–213.

[35] Hulse, C., and Cooper, H. Obama and leaders reach debt deal. *New York Times* (2011).

[36] Jegadeesh, N., and Titman, S. Returns to buying winners and selling losers: Implications for stock market efficiency. *The Journal of Finance 48*, 1 (March 1993), 65–91.

[37] Kenny, R., Hope, B., DeBold, T., and Yang, S. 'Flash Crash' a perfect storm for markets. *Wall Street Journal* (2015).

[38] Khandani, A. E., and Lo, A. W. What happened to the quants in August 2007?

[39] Kirilenko, A., Kyle, A. S., Samadi, M., and Tuzun, T. The Flash Crash: The impact of high frequency trading on an electronic market. Tech. rep., US Commodity Futures Trading Commission, 2014.

[40] Lakonishok, J., Shleifer, A., and Vishny, R. W. Contrarian investment, extrapolation, and risk. *The Journal of Finance 49*, 5 (December 1994), 1541–78.

[41] Lauricella, T., and McKay, P. Dow takes a harrowing 1,010.14-point trip. *Wall Street Journal* (2010).

[42] Lo, A. W. Where do alphas come from?: A measure of the value of active investment management. *Journal of Investment Management 6*, 2 (2008), 1–29.

[43] Lo, A. W., and MacKinlay, A. C. An econometric analysis of nonsynchronous trading. *Journal of Econometrics 45* (1990), 181–211.

[44] Lo, A. W., and MacKinlay, A. C. When are contrarian profits due to stock market overreaction? *Review of Financial Studies 3*, 2 (1990), 175–205.

[45] Lynch, S. Gensler blames the math for 'Flash Crash'. *Wall Street Journal* (2010).

[46] Masset, P. Analysis of financial time-series using Fourier and wavelet methods. *SSRN Electronic Journal* (2008).

[47] McInish, T. H., and Wood, R. A. An analysis of intraday patterns in bid/ask spreads for NYSE stocks. *The Journal of Finance 47*, 2 (June 1992), 753–64.

[48] Moskowitz, T., and Grinblatt, M. Do industries explain momentum? *The Journal of Finance 54*, 4 (August 1999), 1249–90.

[49] Murray, C. As US reaches debt limit, Geithner implements additional extraordinary measures to allow continued funding of government obligations. Tech. rep., US Department of the Treasury, 2011.

[50] Nocera, J. Markets quake, and a 'neutral' strategy slips. *New York Times* (2007).

[51] Novy-Marx, R. The other side of value: The gross profitability premium. *Journal of Financial Economics 108* (2013), 1–28.

[52] Phillips, M. How the robots lost: High-frequency trading's rise and fall. *Bloomberg* (June 2013).

[53] Rua, A. Wavelets in economics. *Banco de Portugal* (2012).

[54] Rubin, R., and Collins, M. How an exclusive hedge fund turbocharged its retirement plan. *Bloomberg* (2015).

[55] Skinner, D. J., and Sloan, R. G. Earnings surprises, growth expectations, and stock returns or don't let an earnings torpedo sink your portfolio. *Review of Accounting Studies 7*, 2 (June 2002), 289–312.

[56] Thomson, D. J. Spectrum estimation and harmonic analysis. *Proceedings of the IEEE 70* (1982), 1055–96.

[57] Twin, A. Brutal day on wall street. *CNN Money* (2007).

[58] Vecellio, G. High frequency trading, accident investigation, and the 6 May 2010 stock market Flash Crash. Tech. rep., MITRE, 2014.

[59] Welch, P. D. The use of Fast Fourier Transform for the estimation of power spectra: A method based on time averaging over short, modified periodograms. *IEEE Transactions on Audio and Electroacoustics AU-15*, 2 (1967), 70–3.

[60] Zuckerman, G., Hagerty, J. R., and Gauthier-Villars, D. Impact of mortgage crisis spreads. *Wall Street Journal* (2007).